Clinical Neurophysiology 130 (2019) 61–76

Contents lists available at ScienceDirect

Clinical Neurophysiology

journal homepage: www.elsevier.com/locate/clinph

Stuttering as a matter of delay in neural activation: A combined TMS/EEG study

Pierpaolo Busan [a,*], Giovanni Del Ben [b], Lucia Roberta Russo [b], Simona Bernardini [c], Giulia Natarelli [d], Giorgio Arcara [a], Paolo Manganotti [e], Piero Paolo Battaglini [b]

[a] Fondazione Ospedale San Camillo IRCCS, via Alberoni 70, 30126 Venice, Italy
[b] B.R.A.I.N. Center for Neuroscience, Department of Life Sciences, University of Trieste, via Fleming 22, 34100 Trieste, Italy
[c] ABC® Balbuzie, Padua, Italy
[d] Department of Developmental and Social Psychology, University of Padua, via Venezia 8, 35100 Padua, Italy
[e] Department of Medical, Surgical and Health Sciences, University of Trieste, Strada di Fiume 447, 34100 Trieste, Italy

ARTICLE INFO

Article history:
Accepted 15 October 2018
Available online 10 November 2018

Keywords:
Supplementary Motor Area
Stuttering
Transcranial Magnetic Stimulation
Combined TMS/EEG
sLORETA
Neural dynamics

HIGHLIGHTS

- Developmental stuttering (DS) relies on dysfunctional neural exchange: the supplementary motor area (SMA) may play a key role.
- We used combined TMS/EEG to investigate functional connectivity of the SMA "complex" in DS.
- Abnormal neural timing in DS is inferred which helps to understand the pathophysiology of DS and develop new treatments.

ABSTRACT

Objective: Brain dynamics in developmental stuttering (DS) are not well understood. The supplementary motor area (SMA) plays a crucial role, since it communicates with regions related to planning/execution of movements, and with sub-cortical regions involved in paced/voluntary acts (such as speech). We used TMS combined with EEG to shed light on connections in DS, stimulating the SMA.
Methods: TMS/EEG was recorded in adult DS and fluent speakers (FS), stimulating the SMA during rest. TMS-evoked potentials and source distribution were evaluated.
Results: Compared to FS, stutterers showed lower activity of neural sources in early time windows: 66–82 ms in SMA, and 91–102 ms in the left inferior frontal cortex and left inferior parietal lobule. Stutterers, however, showed higher activations in later time windows (i.e. from 260–460 ms), in temporal/premotor regions of the right hemisphere.
Conclusions: These findings represent the functional counterpart to known white matter and cortico-basal-thalamo-cortical abnormalities in DS. They also explain how white matter abnormalities and cortico-basal-thalamo-cortical dysfunctions may be associated in DS. Finally, a mechanism is proposed in which compensatory activity of the non-dominant (right) hemisphere is recruited.
Significance: DS may be a disorder of neural timing that appears to be delayed compared to FS; new mechanisms that support stuttering symptoms are inferred; the SMA may be a promising target for neuro-rehabilitation.

Abbreviations: *BA*, Brodmann Area; *DS*, Developmental Stuttering; *EEG*, electroencephalography; *EMG*, electromyography; *FAT*, Frontal Aslant Tract; *FDR*, False Discovery Rate; *FDI*, First Dorsal Interosseous; *FS*, Fluent Speakers; *ICA*, Independent Component Analysis; *MEP*, Motor Evoked Potential; *ROI*, Region of Interest; *RMT*, Resting Motor Threshold; *sLORETA*, Standardized Low Resolution Tomography; *SD*, Standard Deviation; *SSI-4*, Stuttering Severity Instrument-4; *SMA*, Supplementary Motor Area; *TEP*, TMS-Evoked Potential; *TMS*, Transcranial Magnetic Stimulation.

* Corresponding author at: Via Alberoni, 70, ZIP code: 30126, Venice (Lido), Italy.
E-mail addresses: pbusan@units.it (P. Busan), giovanni.delben@phd.units.it (G. Del Ben), giulia.natarelli@phd.unipd.it (G. Natarelli), giorgio.arcara@ospedalesancamillo.net (G. Arcara), pmanganotti@units.it (P. Manganotti), battagli@units.it (P.P. Battaglini).

https://doi.org/10.1016/j.clinph.2018.10.005
1388-2457/

1. Introduction

Developmental stuttering (DS) is a disturbance of the normal rhythm of speech that usually appears in childhood, where affected persons know what they intend to say, but are not able to do it fluently. DS is characterized by dysfluencies such as blocks and repetitions, often associated with movements, especially of the orofacial district. The majority of DS children are able to recover to normal levels, while others remain stutterers into adulthood (persistent DS). DS is related to abnormalities of the central nervous system (Brown et al., 2005; Neef et al., 2015a), and can be considered as a neuro-developmental disorder where speech is mostly affected, considering that it relies on motor skills for planning/execution of articulation (Smith and Weber, 2017). Reduced activity of motor/speech regions has been demonstrated, especially in the left (speech-dominant) hemisphere, during both stuttered and fluent speech, as well as during motor tasks that are not strictly related to speech (Braun et al., 1997) and during rest (Ingham et al., 2012, 1996). On the other hand, frontal/temporal regions of the DS right hemisphere show higher activations (see Etchell et al., 2018 for review). This has been explained as being related to compensation mechanisms (Neumann et al., 2003; Preibisch et al., 2003; Kell et al., 2009), although activity in the right frontal cortex (and its connections with the supplementary motor "complex"-basal ganglia system) may have also a role in the pathophysiology of DS (Neef et al., 2016) within the context of excessive motor inhibition (see also Duann et al., 2009). These "neural markers" may be a consequence of abnormal modulations in intracortical motor networks as demonstrated by TMS experiments (Busan et al., 2017, 2016, 2013, 2009; Neef et al., 2015a, 2015b, 2011; Whillier et al., 2018). They may also be due to defective white matter, especially in brain regions close to and around the left inferior frontal regions, comprising motor/premotor structures, but also in fibers in long-range neural pathways directed toward muscular effectors (Lu et al. 2009; Sommer et al., 2002; Watkins et al., 2008). Finally, other evidence has suggested that DS is related to a defective cortico-basal-thalamo-cortical system (Alm, 2004; Craig-McQuaide et al., 2014) and to dopamine over-activation in the basal ganglia (Wu et al., 1997). These dysfunctions may be at the basis of the speech/motor initiation and rhythm problems that are typically observed in DS (see also Etchell et al., 2014; Smits-Bandstra and De Nil, 2007).

Even if a large amount of research has been carried in DS, questions about the neural mechanisms behind it still remain. For instance, it is not clear if functional deficits, such as white matter abnormalities and cortico-basal-thalamo-cortical dysfunctions, are related to each other or if they represent two different markers. Moreover, uncertainty remains about the temporal neural dynamics of abnormal activations, as well as their connections. In this context, the supplementary motor area (SMA) is a fundamental node: electrical stimulation of this region has been shown to induce stuttering (Penfield and Welch, 1951). Seizures arising from the SMA region have also been related to concomitant stuttering/-gait disturbances (Chung et al., 2004). Stuttering may be the consequence of a damage to the SMA (e.g. Ackermann et al., 1996; Alexander et al., 1987), as well as damage to the thalamus by impairing the cortico-basal-thalamo-cortical system (Abe et al., 1993, 1992). The SMA is a key structure for planning/execution of motor behavior. It is functionally connected with different regions such as the frontal/premotor/sensorimotor, temporo-parietal cortex, sub-cortical regions, and cerebellum, and plays a role in motor/behavioral/cognitive tasks (Narayana et al., 2012). It is subdivided in a "proper", caudal, SMA region, which is strongly connected with structures involved in motor preparation/execution, and in a pre-SMA, rostral, region, which is preferably connected with frontal and "cognitive" regions (decision making and planning of behavior; Zhang et al., 2012). The SMA also has a role in speech control, often in relation to an increase in task demands (Hertrich et al., 2016). This SMA "complex" is involved in cortico-basal-thalamo-cortical networks: it has an active role in tasks such as preparation of voluntary movements (e.g. speech) and in learning of sequential/rhythmic aspects of movements, with particular regard to internally *vs.* externally triggered movements (Nachev et al., 2008; Narayana et al., 2012).

Interestingly, DS may reflect a general impairment in (rhythmic) motor skills (for a review see Etchell et al., 2014), which is related to functional abnormalities in the SMA (e.g. Brown et al., 2005; Etchell et al., 2018). Nevertheless, its role has been often underestimated. Abnormal activity of the SMA in DS was recently suggested to be a possible, adjunctive, "neural marker" of stuttering (see Neef et al., 2015a). In the present work, we aimed to clarify the neural dynamics related to activation of the SMA "complex" in DS. Here, we hypothesize that DS is characterized by different (temporal) neural dynamics and different connections (with respect to fluent speakers [FS]) when the SMA "complex" is activated, with particular attention to neural structures devoted to motor/speech preparation/planning. This is in accordance with the hypotheses that DS might be an impairment of timed neural (sensorimotor) integration, with abnormal communication among different systems. To fulfil this objective, the inductive combination of transcranial magnetic stimulation (TMS) and electroencephalography (EEG) seems to be an appropriate method. TMS/EEG allows direct perturbation of neural networks, measuring how their activity is modulated by a magnetic stimulus. The dynamics and properties of the stimulated tissue may be investigated starting from a basic, "default" state, i.e. when no tasks are requested. Specifically, the analysis of TMS-evoked potentials (TEPs) and reconstruction of their neural source distribution in the temporal domain have been performed to obtain information on the excitability/reactivity of the stimulated cortex and its functional connectivity (see Ilmoniemi, 2016; Miniussi et al., 2013).

2. Materials and methods

2.1. Experimental groups

Twenty-eight right-handed adult males were recruited. Thirteen were persistent DS from childhood (age range 24–47 years, mean 32.9 years, standard deviation [SD] ± 8.3), while 15 were FS (age range 22–48 years, mean 30.4 years, SD ± 7.2). Groups were comparable for age, education, handedness, smoking habits, musical expertise, migraine, and sports habits. Procedures were approved by the regional Ethical Committee of Friuli-Venezia Giulia (Italy). All procedures were in accordance with the Declaration of Helsinki. Participants signed a written informed consent form before the experiment. All participants had no psychiatric/neurologic concerns, other than stuttering in the DS group, and were not taking drugs that act on the central nervous system before experiments. Stuttering was measured with the Stuttering Severity Instrument-4 (SSI-4; Riley, 2009), and was excluded in FS. An audio–video sample of spontaneous speech and a reading passage was requested from each DS participant to measure stuttering severity comprising the percentage of stuttering events, the three longest stuttering events, and physical concomitants. Handedness was evaluated by the Handedness Edinburgh Inventory (Oldfield, 1971).

2.2. TMS

Each participant sat on a chair, at rest, and with open eyes. A tissue cap with an equally spaced 1 cm grid was applied on the scalp.

TMS (Medtronic MagPro R30) was administered on the primary motor cortex using a figure-of-eight coil (C-B60; diameter of every wing 7 cm; biphasic waveform; first phase of current in the coil in posterior-to-anterior direction) to find the position that allowed for the most reliable/reproducible motor evoked potentials (MEPs) from the contralateral first dorsal interosseous (FDI) in both hemispheres. Two Ag/AgCl electrodes were placed on both hands using a tendon-belly montage. The TMS coil was maintained at 45° with respect to the inter-hemispheric fissure, with the handle pointing backwards. TMS was used to detect resting motor threshold (RMT) of FDI by determining the intensity of stimulation that gave contralateral MEPs of about 50 μV in half of stimulations. Electromyography (EMG) was recorded using a digital band pass filtering of 20–2000 Hz (sampling rate 8000 HZ). Resting state was assured by on-line visual inspection of EMG. This procedure was carried out on the primary motor cortex of the left hemisphere and, successively, on the right one. We obtained five contralateral MEPs, from each hemisphere, stimulating at 150% of RMT and recording from FDI, to compare data with those collected in Busan et al. (2013). Thus, the SMA "complex" was roughly marked on the cap using a system based on nasion-inion/bi-auricular distances. We stimulated in/around that region using RMT of the left hemisphere primary motor cortex to verify that it was not possible to evoke bilateral MEPs from FDI, *abductor digiti minimi*, *abductor pollicis brevis*, muscles of forearm, biceps, deltoid, *trapezius*, or *tibialis anteriori*.

2.3. Location of the coil

A neuronavigation system (Visor-2, ANT NEURO B.V., The Netherlands) was used for the correct location of the coil during TMS/EEG recordings. An EEG cap (Electro-Cap B.V., The Netherlands) was placed on the scalp, with sensors for detection of nasion/bi-auricular points. A magnetic resonance model was used for reconstruction: the scalp surface of each participant was reproduced to adapt the model. The SMA "complex" was individuated on the basis of coordinates inferred by Zhang et al. (2012; MNI coordinates: x = 0, y = 6, z = 66; Fig. 1), and marked on the EEG cap. We chose a cortical target that allowed stimulation of the bilateral SMA "complex" (i.e. "proper" SMA and pre-SMA regions).

2.4. Combined TMS/EEG

Participants were sitting in a chair at rest, with the chin placed on a support of a customized table. We recorded the EEG using 31 Ag/AgCl electrodes equally distributed on the scalp (Fig. 1). Two additional electrodes were used as the reference (nose) and ground (below Oz) electrodes. Impedances were always maintained below 5–10 kΩ. Two Ag/AgCl electrodes were placed diagonally around the right eye to record ocular movements/blinks. EEG was recorded by a BASIS BE (EBNeuro, Italy) amplifier and digitally stored using the MIZAR-SIRIUS system (Galileo NT software; EBNeuro, Italy). Sampling rate was 4096 Hz (recording in DC) to limit TMS artefacts on EEG (Veniero et al., 2009). The operational range of the amplifier was set at ±65.5 mV to limit saturation; electrode wires were arranged to limit the effects of the magnetic field on the EEG (Sekiguchi et al., 2011). Raw data were recorded using analogic, no band-pass filtering.

The center of the coil was placed on the individuated scalp position, perpendicularly to the inter-hemispheric fissure, with the handle pointing backwards. Six blocks of stimulation were performed, with each block constituted of 50–60 single pulse trials. The inter-stimulus interval was 2–8 sec. Three blocks were with real TMS, while three blocks were with sham stimulation. Real TMS and sham were always interleaved, and the sequences were randomized. Sham was used to obtain a "model" of the acoustic activity evoked by the pulse, and then "subtracted" from the real TMS during analyses. Participants wore earplugs to limit evoked acoustic activity. Sham TMS was carried out using a piece of wood, about 3 cm in thickness, placed between the scalp and the coil, thus reducing magnetic stimulation to the cortex, but allowing acoustic stimulation (Zanon et al., 2013, 2010). A piece of foam with thickness of about 5 mm was also applied between the coil and scalp to limit somatosensory stimulation (Massimini et al., 2005). The stimulation of a central scalp region allowed limited/avoided artefacts related to muscular activation. Blink reflexes related to TMS delivery were observed during preliminary procedures, with poor adaptation. Thus, participants were asked to remain at rest, with closed eyes during blocks, to limit these artefacts. They were also asked to avoid systematic cognitive activity (such as counting the stimulations). These procedures allowed activation of the SMA "complex" starting from a basic/default con-

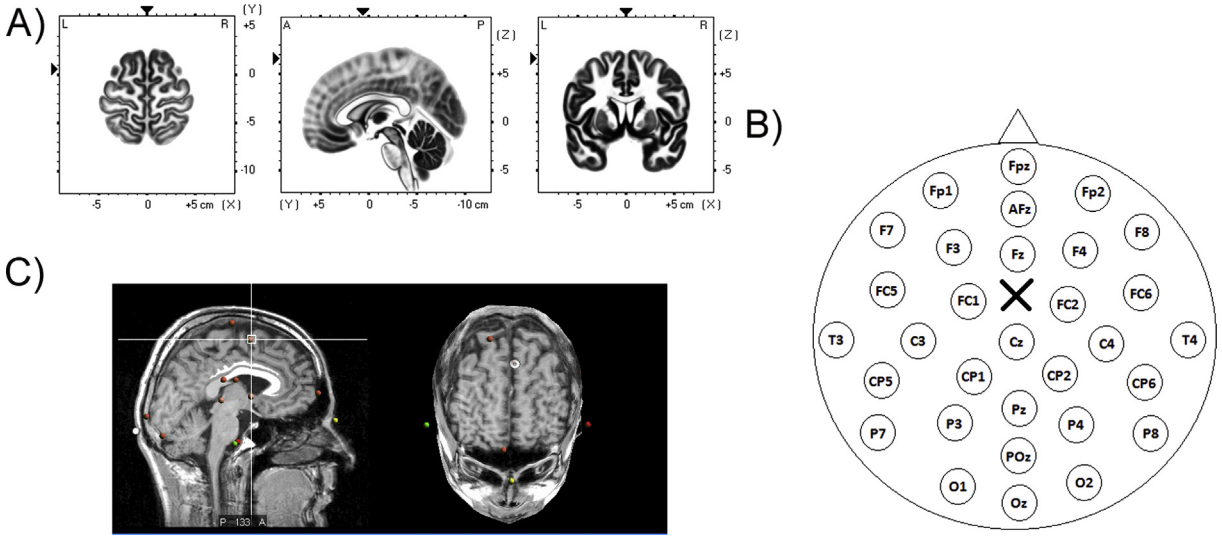

Fig. 1. Representation of stimulation points and recorded EEG electrodes. The coordinates of the cortical target selected in the SMA (Talairach: $x = 0$, $y = 9$, $z = 60$; MNI: $x = 0$, $y = 6$, $z = 66$) is represented on a sLORETA anatomical model of the brain (A) and on a resonance model obtained from neuronavigation (C). Recorded electrodes are also indicated and superimposed on a scalp model (B); the corresponding stimulation point on the scalp is represented.

dition, thus better separating stimulation effects from unspecific ones.

2.5. EEG off-line analysis

EEG traces were analyzed off-line using Neuroscan (Compumedics Neuroscan Inc., El Paso, USA), EEGLAB (Delorme and Makeig, 2004), and erpR (Arcara and Petrova, 2017). Data were digitally filtered by using a low pass IIR filter (edge at 200 Hz). Real TMS and sham were marked to obtain epochs (time window of interest between −200 and 500 ms), locked on TMS delivery. Epochs were inspected to eliminate artefacts (ocular artefacts, blinks, muscular artefacts, drift of the EEG, long-lasting TMS artefacts) and bad electrodes: 22 "singular" electrodes were individuated as bad and interpolated. Data were then used for independent component analysis (ICA; Jung et al., 2000), which is useful to eliminate remaining artefacts. Components were discarded if they represented artefacts only. The interval between −10 and 20 ms with respect to TMS delivery was discarded considering the amount of TMS artefacts, which can corrupt the reliability of ICA. Thus, data were averaged for each participant/condition by using an average reference. A linear de-trend function was applied to reduce the residual influence of the slow recovery of the amplifier after TMS delivery. The resulting TEPs, sub-divided per group (DS *vs.* FS) and condition (real TMS *vs.* sham), were inspected using butterfly plots, where peaks of amplitude allowed the definition of time windows of interest, defined as follows: 36–65 ms, 65–144 ms, 144–256 ms, 256–350 ms, and 350–500 ms.

2.6. Neural source reconstruction (sLORETA)

Temporal windows were used to investigate the distribution of the source reconstruction of TEPs. To obtain source models, we used standardized low resolution electromagnetic tomography (sLORETA; http://www.uzh.ch/keyinst/loreta.htm; Pascual-Marqui, 2002). This algorithm allowed calculation of the standardized, discrete, three-dimensionally distributed, linear, minimum norm inverse solution of evoked potentials. sLORETA was used to reconstruct sources of TEPs obtained in DS and FS during real and sham TMS. To reduce localization errors, a regularization factor was applied by calculating the average of the TEPs signal-to-noise ratio (all electrodes) of each temporal window, based on the estimation of the 20th percentile. We also performed source reconstruction of baselines to control for possible unspecific effects related to the delivery of stimulation.

2.7. Statistical analysis

Data on characteristics of groups (i.e. age, handedness, education, etc.) were compared using parametric (t-statistics/Welch's *t*-test) and/or non-parametric statistics (Mann-Whitney), after checking for normality/homogeneity. TMS motor thresholds and MEPs were analyzed by using similar methods; thresholds were quantified as the percentage of the maximum output of the stimulator; when considering MEPs, peak-to-peak mean amplitudes/areas/latencies were considered. When considering TEPs, hierarchical levels of analysis (compare with Connally et al., 2018) were provided: electrodes placed around the target scalp position (Cz, Fz, FC1, FC2) were considered for descriptive EEG analysis (amplitudes and latencies). Then, an exploratory, uncorrected statistical analysis was performed on all electrodes (t-statistics/Welch's t-test), in which we considered mean amplitudes/areas of TEPs (rectified and not) in the time windows of interest, from 36 to 500 ms. Similar statistics were used for baseline data as a control. When considering source analysis, a voxel-by-voxel comparison was performed for each group (real TMS *vs.* sham) using statistical non-parametrical mapping (Nichols and Holmes, 2002), as available in sLORETA, allowing for conservative corrections for multiple comparisons in space and time. Each analysis was carried out using t-statistics/log of F-ratio to obtain comprehensive patterns of the activations elicited by stimulations. The analysis was performed by considering time frame-by-time frame and the mean neural activity of the time windows of interest (a False Discovery Rate [FDR] procedure was also applied to maximal activation findings, in the case of mean neural activity). As a further correction, we never considered maximal activations that were evident, in a voxel, for less than nine consecutive time frames (≤2 ms, i.e. less than the duration of an action potential; Lodish et al., 2000), for a second level analysis in which we compared DS *vs.* FS (real TMS *vs*. sham). In fact, to reduce intra/intergroup variability, we defined regions-of-interest (ROIs; 15 mm radius), by individuating their center in MNI coordinates and considering the maximal activations of mean and/or time frame-by-time frame analysis. ROIs were bilaterally calculated for real TMS and sham, in each group. Sham activations were "subtracted" from the corresponding real TMS activity, and the results were compared between groups (DS *vs.* fluent speakers; t-statistic/Welch's t-test, depending on variance homogeneity). Comparisons were performed on a time frame-by-time frame basis, and on mean neural activity. The findings resulting in significant activation of at least nine consecutive time frames (>2 ms, i.e. a biologically plausible activation, not less than the duration of an action potential) were considered: they were clustered and a permutation/randomization test (9.999 randomizations) was applied to face with multiple activations (see Premoli et al., 2014; Zanon et al., 2018; an FDR procedure was also applied to findings). Findings were further characterized by providing effect sizes using *Hedges' g*/*Cohen's* $d_{unbiased}$ (Hedges and Olkin, 1985; Cohen, 1988; Ellis, 2010; $0.2 < d_{unbiased} < 0.5$ = small effect; $0.5 < d_{unbiased} < 0.8$ = medium effect; $d_{unbiased} > 0.8$ = large effect). Baseline activity was also compared as a control analysis, between groups and conditions, by applying similar procedures. Significance was always set at $p < 0.05$. Please refer to the Supplementary Material for further methodological details.

3. Results

3.1. Characteristics of groups

Groups did not differ considering age, education, handedness, musical expertise, smoking and sport habits, and migraine. In the DS group, stuttering severity was very mild in two participants, mild in three, moderate in four, and severe in the remaining four. RMTs did not differ between groups and/or hemispheres. FS had higher excitability of the cortico-spinal pathway (MEPs amplitudes/areas) when stimulating the primary motor cortex of the left hemisphere at 150% RMT, and recording from the right FDI, replicating the results of Busan et al. (2013). The results are summarized in Table 1. Please refer to Supplementary Material (Tables S1 and S2) for further characteristics of groups.

3.2. TEPs

When considering TEPs, DS resulted in an average of 93.2 accepted epochs (SD ± 17.8) in the real TMS condition and in 95.7 epochs (SD ± 14.6) in sham. FS resulted in 84.7 accepted epochs (SD ± 15.2) in the real TMS condition and in 89.1 epochs (SD ± 11.8) in sham (no significant differences between conditions and/or groups were seen when considering the number of accepted epochs, $p > 0.1$). When considering electrodes placed around the stimulation point on the scalp (Cz, Fz, FC1, FC2), a series of typical TEPs were observed in both real and sham TMS (Fig. 2; e.g.

Table 1
Main characteristics of groups and participants. Characteristics of groups are indicated by reporting means and SD. Significant differences are in bold, trends toward significance in *italic*.

Characteristic/Groups	DS	FS	p-value
Age	32.9 ± 8.3	30.4 ± 7.2	p = 0.39
Education	17.3 ± 3.6	15.7 ± 2.2	p = 0.34
Handedness	84.4 ± 12.2	85.4 ± 12.6	p = 0.84
Smoke habits	0.24 ± 0.43	0.2 ± 0.41	p = 0.67
Musical instruments expertise	0.26 ± 0.42	0.23 ± 0.41	p = 0.60
Migraine	0.1 ± 0.28	0.07 ± 0.26	p = 0.58
Sport habits	6/7	12/3	p = 0.14
TMS resting motor thresholds	45.9 ± 10.3/ 47.7 ± 9.3	48.8 ± 5.7/ 48.1 ± 7.0	All p > 0.10
MEPs peak-to-peak (μV)	1757.3 ± 1154.1/ 1587.2 ± 1466.6	3161.3 ± 1545.1/ 2287.6 ± 1549.0	**p (DS *vs.* FS LH) = 0.01 (t(26) = 2.688, p = 0.01)** p (DS *vs.* FS RH) = 0.25 p (DS, LH *vs.* RH) = 0.5 *p (FS, LH vs. RH) = 0.06*
MEPs area (V/s)	6688.6 ± 4845.0/ 7310.2 ± 6627.6	12846.4 ± 6768.3/ 8843.6 ± 5868.8	**p (DS *vs.* fl LH) = 0.01 (t(26) = 2.727, p = 0.01)** p (DS *vs.* FS RH) = 0.52 p (DS, LH *vs.* RH) = 0.67 *p (FS, LH* vs. *RH) = 0.052*
MEPs latency (ms)	21.9 ± 1.0/ 21.8 ± 1.3	21.4 ± 1.4/ 21.8 ± 1.4	p (DS *vs.* FS LH) = 0.34 p (DS *vs.* FS RH) = 0.99 p (DS, LH *vs.* RH) = 0.90 *p (FS, LH vs. RH) = 0.08*

Miniussi et al., 2012): a negative component at around 45 ms after TMS (N45), and a positive one at around 60 ms (P60); a negative component at around 100 ms (N100), and a positive one at around 180 ms (P180). A later negative component was also evident at around 280 ms (N280). Thus, TEP components (butterfly plots) allowed identification of five time windows of interest: 36–65 ms, 65–144 ms, 144–256 ms, 256–350 ms, and 350–500 ms. Detailed characterization of TEPs, and exploratory statistics are reported in the Supplementary Material (Tables S3 and S4). In general, the analysis resulted in differences in fronto-centro-parietal electrodes, in both hemispheres, with higher neural activity mainly evident in FS, especially in the first 150 ms after TMS delivery. On the other hand, higher neural activity in DS was recorded starting from about 150 ms after TMS.

3.3. Neural source reconstruction

In both FS and DS, real TMS always resulted in higher activations than sham. Significant neural activations reported by FS were, in general, wider and more distributed than those reported by DS. Groups were characterized by different neural dynamics of activity (in terms of activated brain regions and the timing of activation) related to the stimulation of the SMA "complex". This allowed definition of specific ROIs, exclusive for each group and time window, which were useful for neural source reconstruction comparisons between groups (see Tables 2 and 3, Figs. 3 and 4, and Tables S5, S6, and S7; time frame-by-time frame analysis in the Supplementary Material).

3.3.1. Neural source reconstruction in FS

FS (mean neural activity) resulted in the maximal activation of a region centered in the right superior frontal gyrus (36–65 ms; BAs 9 and 11) and of regions centered in the right parietal lobe (65–144 ms; BA 40) and left prefrontal cortex (65–144 ms; BA 11). At 144–256 ms after TMS, the maximal activation of regions surrounding the right middle temporal cortex (BA 21) and left superior parietal lobe (BA 7) was evident. The maximal activation of regions around the right postcentral gyrus (BA 43) and the right frontal cortex (BA 6) was evident at 256–350 ms. Regions around the left middle temporal cortex (BA 21) and right supramarginal gyrus (BA 40) were maximally activated at 350–500 ms after TMS.

3.3.2. Neural source reconstruction in DS

DS (mean neural activity) resulted in the maximal activation of a region centered in the left inferior frontal and precentral gyrus (36–65 ms; BA 6), followed by the maximal activation of regions centered in the right precentral gyrus and the right prefrontal cortex (65–144 ms; BAs 6 and BA 10, respectively). Successively (144–256 ms), the maximal activation of regions centered in the left frontal cortex was evident (BAs 6 and 46), as well as activations in regions close to the left temporal cortex (256–350 ms; BA 22) and right superior frontal gyrus (256–350 ms; BA 6). Finally, at 350–500 ms, DS resulted in the maximal activation of regions centered in the right temporal cortex (BA 38) and in the right frontal cortex (BA 6).

3.4. ROI analysis: DS vs. FS

Analyses of mean neural activity for each group allowed identification of 4 ROIs for each time window, which were considered bilaterally. ROIs are summarized in Fig. 5 and Table S7 (Supplementary Material). All statistics and the results are summarized in Table 4 and Fig. 6.

3.4.1. FS > DS in the first 150 ms after TMS

A significant difference (lower activation in DS than in FS) was evident in the ROI centered on the SMA (superior frontal gyrus, BA 6) between 66–71 ms and between 75–82 ms. A similar difference in a region centered in the left precentral gyrus (BA 6), in a successive time window between 91–102 ms was evident (a trend was also observed in the mean neural activity of the entire window, 65–144 ms). Next, a significant difference was seen in the region centered in the left inferior parietal lobule (BA 40), with higher activity in FS (99–101 ms). Successively, the analysis resulted in the activation of parietal regions of the right hemisphere (center of the ROI in superior parietal lobule, BA 7; higher activation in FS *vs.* DS) in a time between 149 and 152 ms. Finally (and later in time), DS resulted in lower activation of the region centered in the left middle temporal gyrus (BA 21) between 369 and 374 ms.

3.4.2. DS > FS starting from 250 ms after TMS

Given the above, the stuttering brain seemed to "react" to previous lacking of activation: significant differences were observed at

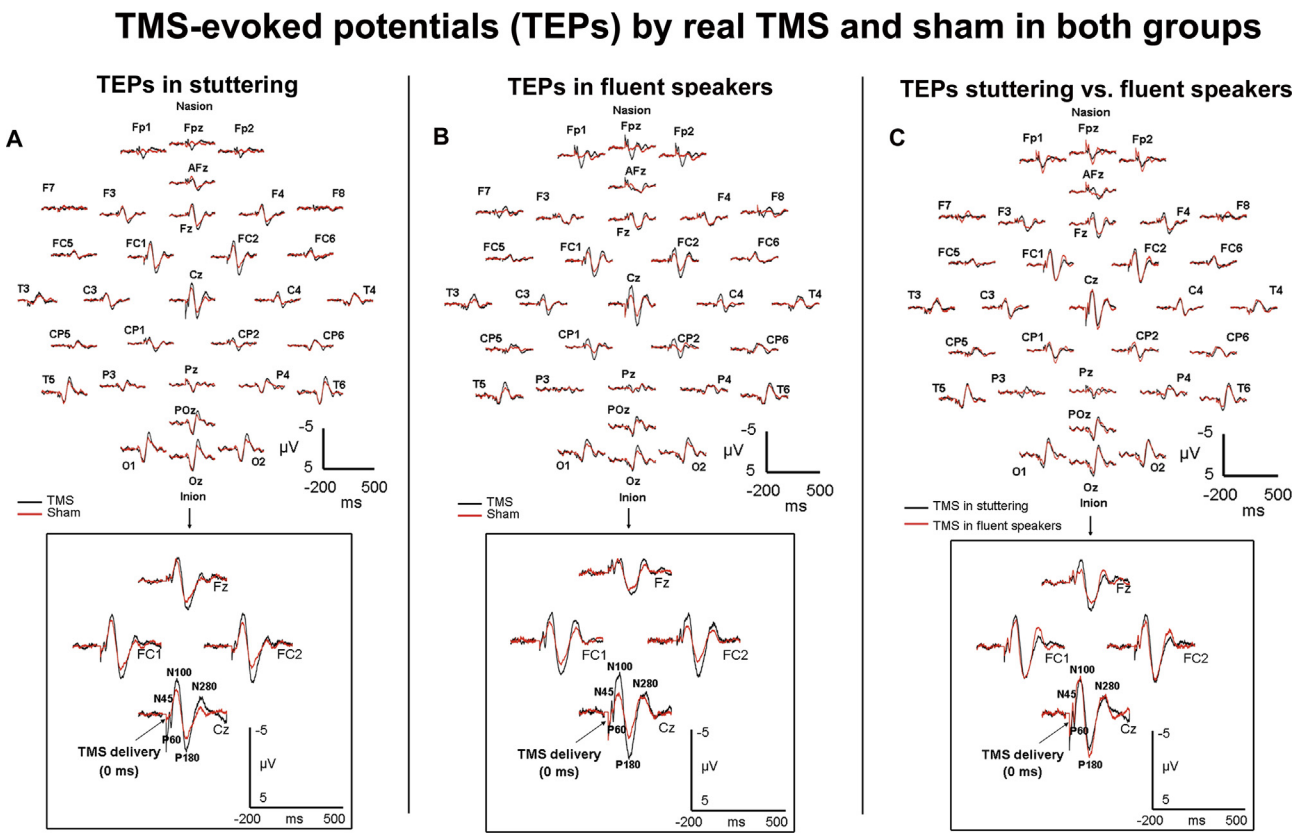

Fig. 2. Representation of TMS-evoked potentials in fluent speakers and in the stuttering group. (A) Real TMS vs. sham in the stuttering group; (B) real TMS vs. sham in the fluent speakers group; (C) comparison of real TMS in the stuttering and fluent speaker groups. In each panel, electrodes placed around the coil are highlighted to represent components of TMS-evoked potentials.

263–268 ms and at 273–280 ms in the right temporal cortex (ROI centered in the superior temporal gyrus; BA 22), with higher activity in DS than in FS. This was also observed when considering a ROI centered in the right parietal cortex (postcentral gyrus; BA 43), with activations that resulted higher in DS, in a time between 265 and 268 ms, and between 274 and 277 ms. Closer regions of the right hemisphere (ROI centered in the right middle temporal gyrus, BA 21) were more activated in DS at 378–380 ms. Similarly, the region centered in the right superior temporal gyrus (BA 38) was also more activated in stuttering in a time between 378 and 380 ms, as well as in a time between 425 and 427 ms. Finally, DS resulted in a higher neural activity in regions around the right middle frontal gyrus (BA 6) in a time between 454 and 462 ms. This was similarly observed in the cortical surface surrounding the right superior frontal gyrus (BA 6), at 456–463 ms (DS more activated than FS), in a region that roughly corresponded to the initially stimulated SMA "complex".

When considering ROIs obtained from time frame-by-time frame analyses, there were no significant differences in either group, and thus further details are not specified.

3.5. Control analysis

Findings obtained from analysis of ROIs were used to verify whether similar findings were evident when considering baseline activity (from −200 to −10 ms before TMS delivery). No significant differences were present between groups.

4. Discussion

4.1. Summary of results

The present findings suggest that adults with persistent DS are characterized by different neural dynamics in terms of time and in brain localization. The DS brain was characterized by lower "reactivity" after the stimulation of the SMA "complex". TEPs resulted in (exploratory) differences in specific electrodes: DS resulted in lower activation of fronto-parietal electrodes, especially of the left hemisphere, until about 150 ms after TMS (see Supplementary Material). DS resulted in higher responses after this time. "Typical" TEPs were observed in real/sham TMS (Miniussi et al., 2012): their functional meaning is not fully clarified (Hill et al., 2016; Miniussi et al., 2012) but, for example, N45 is modulated by GABA-ergic activity (Premoli et al., 2014). N100 (TMS on the primary motor cortex) is modulated by motor preparation, again reflecting inhibitory activity of interneurons (Nikulin et al., 2003; Premoli et al., 2014). This may also be evident in non-motor regions (Rogasch et al., 2015). TEPs are further modulated by the acoustic response to TMS (e.g. Nikulin et al., 1999) suggesting that components are represented by different neuronal sources. Thus, neural source reconstruction of TEPs allows identification of differences in neural dynamics, comparing DS and FS. The SMA "complex" of DS "reacted" with a lower activation (*vs.* FS) at about 65–80 ms after TMS. This pattern continued, at about 90–100 ms, in motor planning regions of the left hemisphere (precentral gyrus [BA 6], as well as in the left inferior parietal lobule [BA 40]). This was counter-

Table 2
Mean neural activations obtained comparing real TMS *vs.* sham in fluent speakers. Mean neural activations obtained comparing real TMS *vs.* sham in fluent speakers, in the different time windows of interest, are reported.

Mean neural activity (sLORETA)						
Time window of interest	Maximal activation (BA; MNI x, y, z coordinates)		Other brain regions activated (BA)		Total number of voxels	
	t-statistic	Log of ratio of averages	t-statistic	Log of ratio of averages	t-statistic	log of ratio of averages
36–65 ms	Right superior frontal gyrus (9R; 45, 35, 35)	Right superior frontal gyrus (11R; 30, 55, −15)	4R, 6L/R, 8L/R, 9L, 10L/R, 11L/R, 13R, 20R, 21R, 22L/R, 24L/R, 25L/R, 28R, 32L/R, 33L/R, 34R, 36R, 38R, 42R, 43R, 44L/R, 45R, 46L/R, 47R	9L/R, 10L/R, 11L/R, 13R, 20R, 21R, 22R, 24L/R, 25L/R, 28R, 32L/R, 34R, 36R, 38R, 44R, 45R, 46L/R, 47L/R	1317 (*max stat.* p < 0.0002)	1024 (*max stat.* p < 0.0002)
65–144 ms	Right inferior parietal lobule (40R; 65, −30, 40)	Left rectal gyrus (11L; −5, 55, 25)	1L/R, 2L/R, 3L/R, 4L/R, 5L/R, 6L/R, 7L/R, 8L/R, 9L/R, 10L/R, 11L/R, 13L/R, 18R, 19R, 20L/R, 21L/R, 22L/R, 23L/R, 24L/R, 25L/R, 27R, 28L/R, 30R, 31L/R, 32L/R, 33L/R, 34L/R, 35L/R, 36L/R, 37R, 38L/R, 39R, 40L, 41L/R, 42L/R, 43L/R, 44L/R, 45L/R, 46L/R, 47L/R	3L/R, 4L/R, 5L/R, 6L/R, 7L/R, 8L/R, 9L/R, 10L/R, 11R, 13L/R, 20L/R, 21L/R, 22L, 24L/R, 25L/R, 28L/R, 31L/R, 32L/R, 33L/R, 34L/R, 36R, 38L/R, 44L/R, 45L/R, 46L/R, 47L/R	4980 (*max stat.* p < 0.0002)	2429 (*max stat.* p < 0.0002)
144–256 ms	Right middle temporal gyrus (21R; 65, −50, −10)	Left superior parietal lobule (7L; −30, −70, 55)	1L/R, 2L/R, 3L/R, 4L/R, 5L/R, 6L/R, 7L/R, 8L/R, 9L/R, 11L/R, 13L/R, 17L/R, 18L/R, 19L/R, 20L/R, 21L, 22L/R, 23L/R, 24L/R, 25L/R, 27L/R, 28L/R, 29L/R, 30L/R, 31L/R, 32L/R, 33L/R, 34L/R, 35L/R, 36L/R, 37L/R, 38L/R, 39L/R, 40L/R, 41L/R, 42L/R, 43L/R, 44L/R, 45L/R, 46L/R, 47L/R	1L/R, 2L/R, 3L/R, 4L/R, 5L/R, 6L/R, 7R, 8L/R, 9L/R, 13L, 18L, 19L/R, 20L, 22L, 23L/R, 24L/R, 27L/R, 28L, 29L/R, 30L/R, 31L/R, 32L/R, 33L/R, 35L, 36L, 37L, 39L/R, 40L/R, 41L, 42L, 43L, 44L, 45L, 46L	5194 (*max stat.* p = 0.0006)	2503 (*max stat.* p = 0.0018)
256–350 ms	Right postcentral gyrus (43R; 65, −15, 15)	Right middle frontal gyrus (6R; 30, 10, 65)	1R, 2R, 3R, 4R, 6R, 10L/R, 11L/R, 21R, 22R, 37R, 40R, 42R	NA	194 (*max stat.* p = 0.01)	1 (*max stat.* p = 0.023)
350–500 ms	Left middle temporal gyrus (21L; −65, −15, −5)	Right supramarginal gyrus (40R; 65, −50, 30)	1L/R, 2L/R, 3L/R, 4L/R, 5R, 6L/R, 8R, 9L/R, 13L/R, 20L/R, 21R, 22L/R, 24R, 31R, 37R, 38L/R, 39L/R, 40L/R, 41L/R, 42L/R, 43L/R, 44L/R, 45L/R, 46R, 47L/R	1L/R, 2L/R, 3L/R, 4L/R, 6L/R, 8R, 9R, 13R, 20L/R, 21L/R, 22L/R, 24R, 31R, 39R, 40L, 41L/R, 42L/R, 43L/R, 44R, 45R	1637 (*max stat.* p = 0.0018)	692 (*max stat.* p = 0.004)

Table 3
Mean neural activations obtained comparing real TMS and sham in the stuttering group. Mean neural activations obtained comparing real TMS and sham in the stuttering group, in the different time windows of interest, are reported.

Mean neural activity (sLORETA)						
Time window of interest	Maximal activation (BA; MNI x, y, z coordinates)		Other brain regions activated (BA; left/right)		Total number of voxels	
	t-statistic	Log of ratio of averages	t-statistic	Log of ratio of averages	t-statistic	log of ratio of averages
36–65 ms	Left inferior frontal gyrus (6L; −60, 10, 30)	Left precentral gyrus (6L; −65, −5, 25)	1L, 2L, 3L, 4L, 8L, 9L, 13L, 20L, 21L, 22L, 36L, 37L, 38L, 40L, 41L, 42L, 43L, 44L, 45L, 46L, 47L	3L, 4L, 9L, 22L, 43L, 44L	610 (*max stat.* p = 0.0014)	21 (*max stat.* p = 0.026)
65–144 ms	Right precentral gyrus (6R; 60, −5, 35)	Right medial frontal gyrus (10R; 5, 65, 20)	1L/R, 2L/R, 3L/R, 4L/R, 5L/R, 6L, 7L/R, 8L/R, 9L/R, 13R, 20R, 21R, 22R, 23L/R, 24L/R, 25R, 27R, 28R, 31L/R, 32L/R, 33L/R, 34R, 35R, 36R, 38R, 40L/R, 41R, 42R, 43R, 44R, 45R, 46L/R, 47R	9L/R, 10L, 11L/R, 46L	2369 (*max stat.* p < 0.0002)	163 (*max stat.* p = 0.0006)
144–256 ms	Left precentral gyrus (6L; −65, −5, 30)	Left middle frontal gyrus (46L; −45, 45, 20)	1L/R, 2L/R, 3L/R, 4L/R, 5L/R, 6R, 7L/R, 8L/R, 9L/R, 10L/R, 11L/R, 13L/R, 17L/R, 18L/R, 19L/R, 20L/R, 21L/R, 22L/R, 23L/R, 24L/R, 25L/R, 27L/R, 28L/R, 29L/R, 30L/R, 31L/R, 32L/R, 33L/R, 34L/R, 35L/R, 36L/R, 37L/R, 38L/R, 39L/R, 40L/R, 41L/R, 42L/R, 43L/R, 44L/R, 45L/R, 46L/R, 47L/R	6L/R, 8R, 9L/R, 10L/R, 11L/R, 19R, 32L/R, 45L, 46R	4920 (*max stat.* p = 0.0006)	460 (*max stat.* p = 0.0016)
256–350 ms	Left superior temporal gyrus (22L; −65, −15, 5)	Right superior frontal gyrus (6R; 20, 5, 70)	3L/R, 4L/R, 6L/R, 9L, 21L/R, 22R, 38R, 40L/R, 42L/R, 43L/R, 44L/R, 45L/R, 47L/R	1L, 3L/R, 4L/R, 6L, 8L/R, 9L/R, 24L/R, 31L/R, 32L/R	185 (*max stat.* p = 0.012)	665 (*max stat.* p = 0.006)
350–500 ms	Right superior temporal gyrus (38R; 55, 10, −15)	Right middle frontal gyrus (6R; 30, 10, 65)	1R, 2R, 3L/R, 4L/R, 6L/R, 8R, 9L/R, 10R, 11R, 13L/R, 20R, 21L/R, 22L/R, 24R, 25L/R, 27R, 28R, 32R, 33R, 34R, 35R, 36R, 37R, 38L, 39R, 40R, 41R, 42L/R, 43L/R, 44L/R, 45L/R, 46L/R, 47L/R	6L, 8R, 9R, 24R, 32R	1598 (*max stat.* p = 0.0012)	188 (*max stat.* p = 0.0028)

acted by the later recruitment of regions of the right temporal cortex, at times between 260–280 ms and 380–460 ms after TMS. DS activated the right premotor cortex and right hemisphere regions (very close to the stimulated SMA "complex") at about 455–460 ms after TMS. The excitability of the left primary motor cortex (MEPs from hand muscles) was lower in DS, with a lower dominance of the left hemisphere.

These findings suggest that DS is a disturbance where dysfunctional activation/communication among neural networks is involved, not only related to speech, but also to more general motor programming. DS consistently resulted in atypical activation of brain regions such as the left inferior frontal regions and the bilateral temporal cortex, and also showed abnormalities in connectivity (e.g. to the SMA; see Etchell et al., 2018). As a consequence, the present findings will be discussed by considering a "network" point of view, by following the "temporal" flow of the present results. A comparison of present findings with previous TMS and/or EEG works in DS, and with computational models of DS, is present in the Supplementary Material.

4.2. SMA "complex" and DS: the role of motor timing in the cortico-basal-thalamo-cortical network

The SMA has only recently been proposed as a "neural marker" of DS (see Belyk et al., 2015; Budde et al., 2014; Neef et al., 2015a) in addition to "classical" markers such as the lower activity of speech/motor regions of the left hemisphere and higher activity of the homologue regions of the right one (Brown et al., 2005; Budde et al., 2014). Herein, we show that, after magnetic stimulus, the SMA in DS is not able to activate as it does in FS, and this might negatively influence the successive activation of the left hemisphere fronto-temporo-parietal network. The SMA is part of a cortico-striato-thalamo-cortical system that has a role in self-initiated motor programs. The SMA is involved in the temporal organization of sequential motor tasks for early planning and coding of multiple movements (Cona and Semenza, 2017; Coull et al., 2015; Nakamura et al., 1998; Tanji and Shima, 1996, 1994), as well as in the update of motor plans in subsequent movements (Shima et al., 1996). It has a role in monitoring motor performance (Shima and Tanji, 2006) and in initiating actions on the basis of self-generated temporal estimates (Mita et al., 2009). This region has been shown to be part of a speech production system, together with premotor and inferior frontal regions, even in DS (Brown et al., 2005; Fox et al., 2000). Increased activations in regions such as the basal ganglia, sensorimotor regions, and the SMA "complex", during rest, dysfluencies, speech tasks, and/or non-speech movements, may be observed in DS, especially in the right hemisphere, in contrast to lower activations in similar regions of the left one (see Etchell et al., 2018 for an exhaustive review). Qiao et al. (2017) reported abnormal functional connectivity in DS in the SMA "complex" and primary motor cortex, as well as in inferior frontal regions (especially in the left hemisphere) and basal ganglia. This was most evident for information flowing from inferior frontal cortex to the SMA, and from the SMA to premotor cortex; this was also true when considering neural flow from basal ganglia to the cortex and vice versa. The lower activations of SMA reported herein support the vision that DS is related to defective activation of a system used to control an "*internal timing network*", involved in volitional movements (such as speech), in contrast to an "*external timing network*", more involved in movements that rely on external/sensorial cues (Alm, 2004; Avanzino et al., 2016; Etchell et al., 2014). A "delay" in the cortico-basal-thalamo-cortical system may result in an insufficient movement initiation (compare with Alm, 2004; Civier et al., 2013; Connally et al., 2018). The present observation of an initial lack of activation in the SMA "complex", followed by higher activations of premotor regions of the right

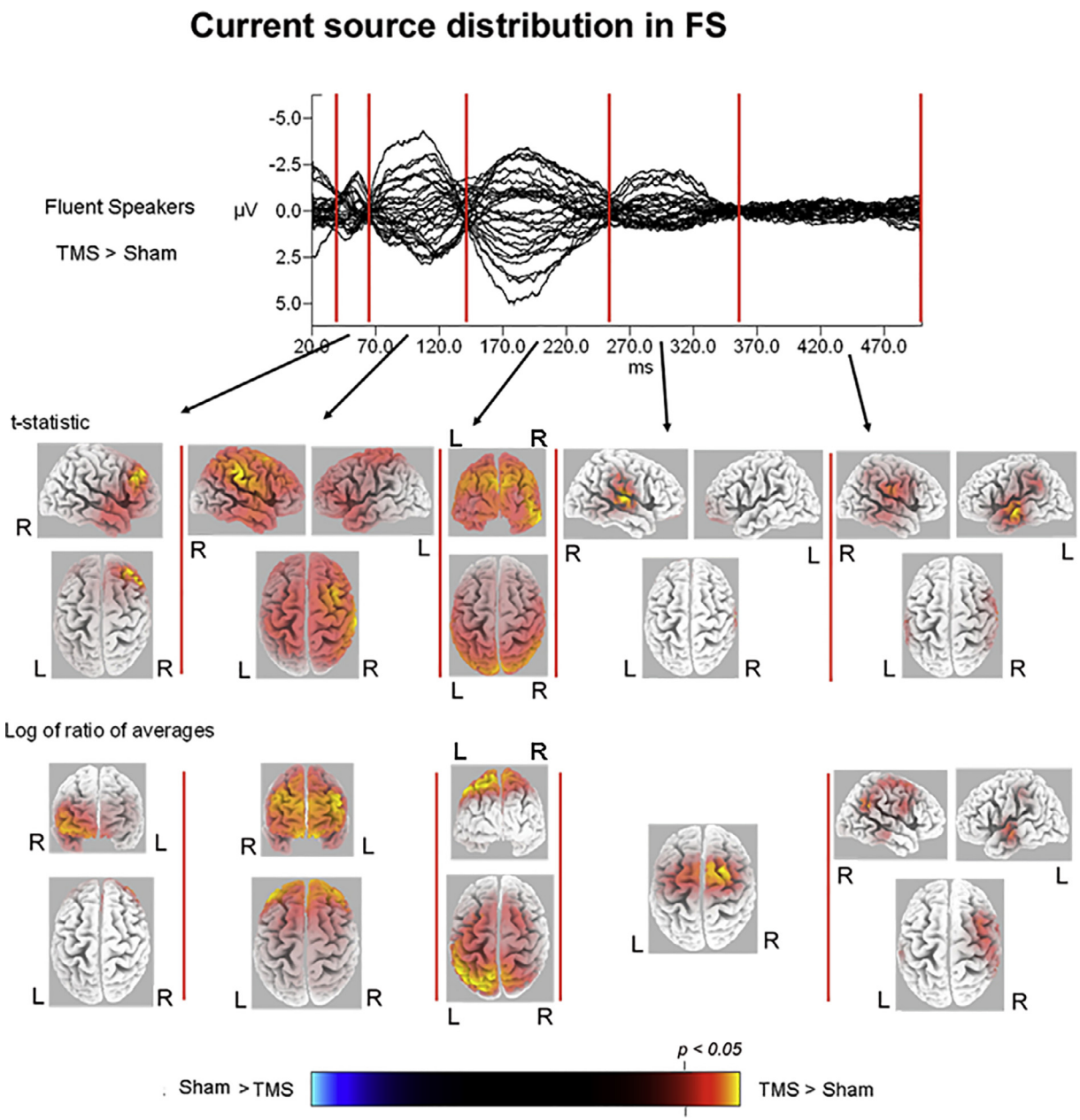

Fig. 3. Representation of significant neural sources in the fluent speakers group comparing real TMS to sham in the different time windows of interest (mean neural activity). Significant differences between real TMS and sham conditions in fluent speakers are reported with indication of the involved time windows of interest. For each time window of interest, sources obtained by t-statistic and log of F-ratio are reported. Red/yellow colors indicate that real TMS resulted in higher activation than sham. Activations are reported using relative scales to represent voxels that were significantly activated ($p < 0.05$, corrected); L = left hemisphere, R = right hemisphere. (For interpretation of the references to colour in this figure legend, the reader is referred to the web version of this article.)

hemisphere after about 400 ms from it, sustain this possibility. Basal ganglia dysfunction is also commonly reported in DS (Alm, 2004; Craig-McQuaide et al., 2014), resulting in lower connectivity of related circuits, including SMA (Chang and Zhu, 2013; Chang et al., 2016) and influencing motor and/or large-scale networks (Cantello et al., 2002; Lu et al., 2010b, 2009; Metzger et al., 2018; Yang et al., 2016; Ziemann et al., 1997). Smaller cerebral volumes may be evident after basal ganglia lesions in the SMA (Exner et al., 2002). On the other hand, children recovering from DS show a decreased gyrification of the SMA, suggesting a decreased local connectivity and/or a better synaptic pruning of longer neural circuits favouring fluency (Garnett et al., 2018).

More importantly, SMA is strongly connected with regions of the inferior frontal gyrus, which are part of the motor pathways, through the frontal aslant tract (FAT): Kronfeld-Duenias et al. (2016) suggested that stuttering (i.e. speech fluency) is related to fiber integrity of the FAT. Misaghi et al. (2018) reported higher fractional anisotropy and higher axial diffusivity in the right FAT of children who stutter. The FAT is involved in motor/speech production and initiation (Kinoshita et al., 2015): Kemerdere et al. (2016) observed that electro-stimulation of the left FAT in FS during neurosurgery caused stuttering, while Neef et al. (2018) reported that stuttering severity may be positively related with the "strength" of neural pathways such as the right FAT and/or projections of the right precentral sulcus. A lower functionality of this connection (e.g. reduced synchrony), in the left hemisphere, may be related with slow transfer of neural information and/or abnormal communication between regions such as the SMA and inferior

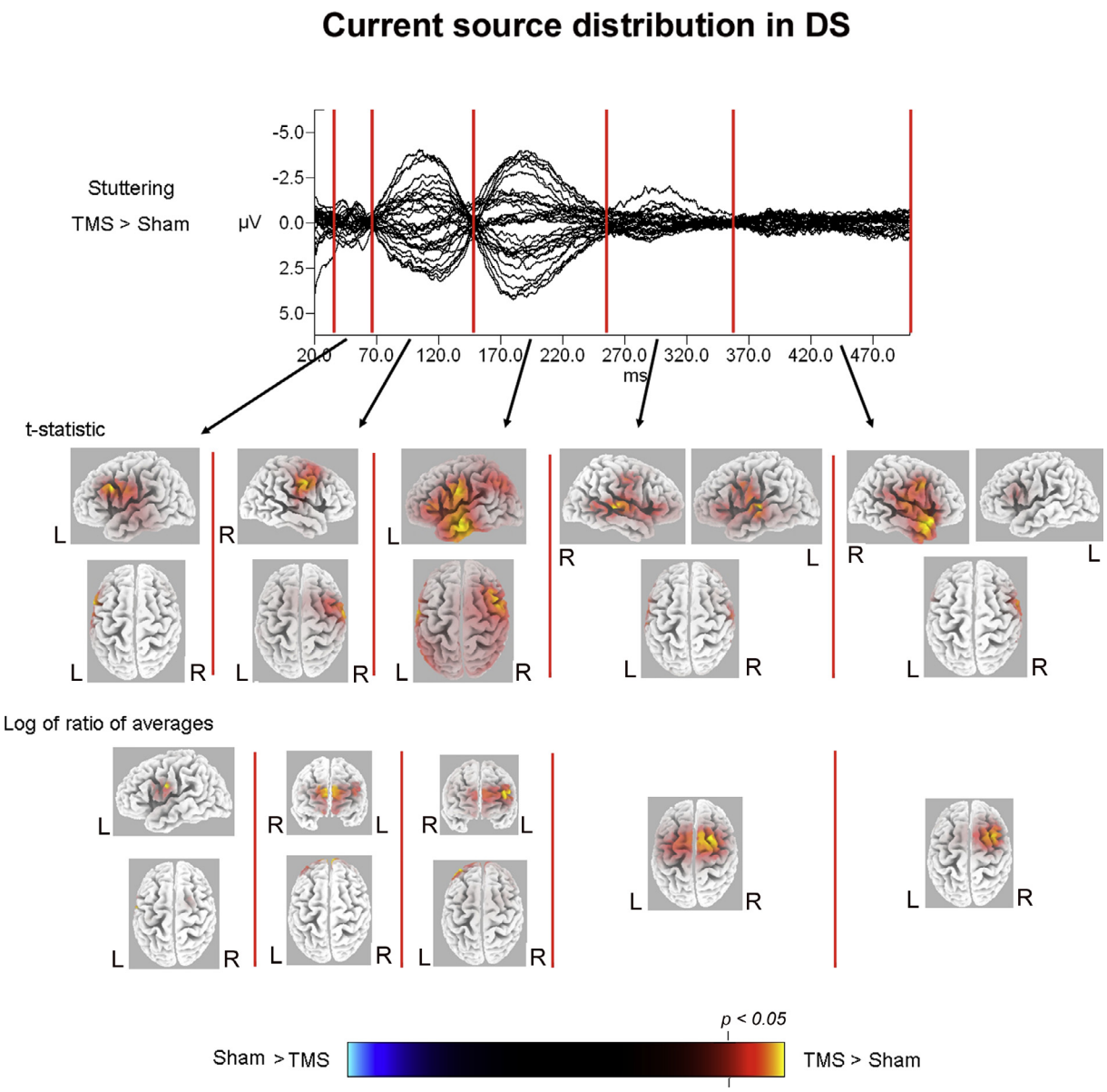

Fig. 4. Representation of significant neural sources highlighted in the stuttering group comparing real TMS to sham in the different time windows of interest (mean neural activity). Significant differences between real TMS and sham conditions in stuttering are reported with indication of the involved time windows of interest. For each time window of interest, sources obtained by t-statistic and log of F-ratio are reported. Red/yellow colors indicate that real TMS resulted in higher activation than sham. Activations are reported by using relative scales, to represent voxels that were significantly activated ($p < 0.05$, corrected); L = left hemisphere, R = right hemisphere. (For interpretation of the references to colour in this figure legend, the reader is referred to the web version of this article.)

frontal cortex (devoted to speech/motor control), impairing planning/initiation/control of motor acts (compare also with Kronfeld-Duenias et al., 2016). This is also supported by the present findings, where "insufficient" activation of the SMA "complex", after TMS delivery, was followed by a similar "insufficient" activation of frontal/premotor regions of the left hemisphere around the inferior frontal cortex. The potential role of the fronto-striatal tract should also be considered when interpreting the present findings (see Kinoshita et al., 2015).

4.3. Relation of the present findings with deficits in left inferior frontal regions and white matter

Successive to the lower activation of the SMA "complex", after TMS delivery, our findings show that the premotor/inferior frontal regions of the left hemisphere are also under-activated in DS, and accompanied by similar under-activation of the left parietal cortex, which is compatible with the suggestion that DS is an impairment in mechanisms of planning/execution of movement and speech (Civier et al. 2013, 2010; Howell, 2004; Lu et al., 2010a; Max et al., 2004). Previous research in DS consistently reported diffuse anatomo-functional abnormalities, which were especially evident in regions such as the bilateral inferior frontal cortex, premotor areas, medial frontal regions, temporal cortex, and sensorimotor regions, as well as their connections, especially (but not exclusively) during speech production (often in relation with stuttering severity; see Etchell et al., 2018, for a recent review). The (left) inferior frontal cortex has a role in several functions ranging from action to rhythm processing and cognitive control (see Neef et al., 2016, for a review related to DS). While the anterior part is more related to cognition, the posterior regions may be more related to motor/rhythmic skills (Clos et al., 2013), even in connec-

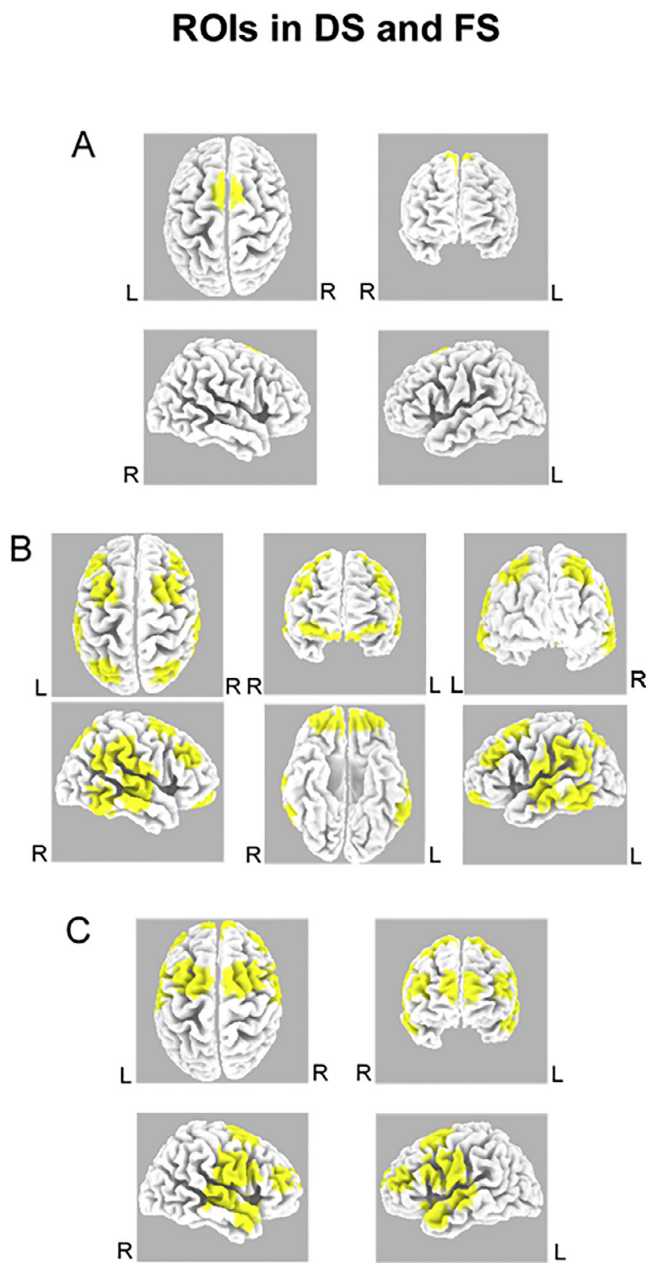

Fig. 5. Representation of region of interests (ROIs) as individuated by analysis of mean neural activity of real TMS *vs.* sham, in the different time windows of interest, in fluent speakers and in stutterers. (A) ROI corresponding to stimulation point; (B) ROIs obtained from source analysis in fluent speakers; (C) ROIs obtained from source analysis in stuttering. Please compare with Table S6 (Supplementary Material) for information about the different time windows of interest.

tion with the SMA "complex" (see Neef et al., 2016), as requested by the production of fluent speech (compare with Restle et al., 2012). It has been clearly demonstrated that the left inferior/medial frontal cortex of DS is characterized by reduced activation, especially (but not exclusively) in speech-related contexts (e.g. Desai et al., 2017; Neef et al., 2016; Watkins et al., 2008), by reduced resting state connectivity (Lu et al., 2012) and/or by the presence of lower volume/thickness (Beal et al., 2013; Chang et al., 2008; Garnett et al., 2018; Kell et al., 2009; Lu et al., 2012, 2010b), even in (negative) relation with stuttering severity (Kell et al., 2009). Neef et al. (2016) demonstrated that DS is linked to the reduced activation of left inferior frontal regions, and, specifically, to impaired coupling between them and the left inferior parietal lobule (see also Lu et al., 2010a), in agreement with the present observations. Those authors stated that this network may be useful to implement planning of speech movements (see also Hickok et al., 2009) and in managing motor/rhythmic skills. They further suggest that impaired connectivity of these structures with the left superior frontal gyrus (i.e. SMA) may be at the basis of the functional impairments in DS (see also Chang et al., 2011; Neef et al., 2015a). In fact, improvement and/or spontaneous recovery of DS has been associated with functional changes in the dynamics of these networks, also comprising the temporal cortex (e.g. Civier et al., 2015; Kell et al., 2018, 2009; Stager et al., 2003). Compatibly, abnormal and/or lower connectivity/white matter integrity in inferior frontal regions, premotor cortex and in motor areas, also comprising the representation of speech muscles such as tongue and larynx, as well as cortico-spinal/cortico-bulbar fibers (especially in the left hemisphere), is a common finding in DS, involving pathways and regions that are useful for speech integration such as the superior longitudinal fasciculus, the arcuate fasciculus, and the angular gyrus (Cai et al., 2014b; Chang et al., 2011, 2008; Connally et al., 2014; Cykowski et al., 2010; Sommer et al., 2002; Watkins et al., 2008; see also Cieslak et al., 2015; Chang et al., 2015; Chow and Chang, 2017; Neef et al., 2015a). The maturational patterns of pars opercularis may be different, in DS, when considering gray matter (Beal et al., 2015): children with DS had less gray matter volume in brain areas such as the inferior frontal regions (Beal et al., 2013), while the persistent stutterers were characterized by slower growth of white matter even in brain regions such as the left arcuate fasciculus and corpus callosum (Chow and Chang, 2017). Generally, this evidence may result in lower excitability of the left primary motor cortex (Busan et al., 2017, 2016, 2013; Neef et al., 2015b; Whillier et al., 2018; Neef et al., 2015b; Whillier et al., 2018). Thus, the here reported lower activity of the left premotor/inferior frontal regions (and parietal cortex) may be the consequence, from a temporal point of view, of under-activation starting from the SMA, likely driven through the FAT. However, a mutual influence is more likely: children with persistent DS show a reduced cortical thickness of the left motor/premotor regions; such a difference is not evident in SMA (Garnett et al., 2018).

4.4. Right-hemispheric activations: an attempt to recover proper neural timing

Starting from about 250 ms after TMS, the stuttering brain "react" to the initial lack of activation, and is consistently more activated than FS, albeit in the right hemisphere. This was evident especially in temporal regions, such as in the superior and middle temporal cortex, as well as in post-central regions. These higher activations extinguished within 460 ms after TMS, when higher activity was evident in motor regions of the right hemisphere, corresponding to the right dorsal premotor cortex and to the initially stimulated SMA "complex". Higher activation of fronto-temporal regions of the right hemisphere has been consistently reported in DS research (Brown et al., 2005; Budde et al., 2014; Ingham et al., 2012; Neef et al., 2015a). However, the functional meaning of this activity has not been fully clarified. It has often been suggested it should have a compensatory role, trying to overcome difficulties of similar regions of the left one (Kell et al., 2009; Neumann et al., 2005, 2003; Preibisch et al., 2003). Hartwigsen et al. (2013) demonstrated that right frontal regions were able to support adaptive plasticity in speech tasks after perturbation of the left inferior frontal cortex. Braun et al. (1997) reported that DS was positively related to the activity of the left hemisphere, while a negative correlation was evident in the right one (see also Fox et al., 2000). Chang et al. (2011) reported greater connectivity in DS between the inferior frontal cortex and right sensorimotor

regions, while Chang and Zhu (2013) reported greater connectivity of the latter with the left SMA and basal ganglia. On the other hand, a pathological role of frontal activity in the right hemisphere has been suggested, in terms of excessive inhibitory activity on normal motor processes (Neef et al., 2016). In the present work, the consequential activations of temporal regions and, finally, of motor associative regions (after a lack of activity in similar motor regions of the left hemisphere) sustain the vision of a compensative role of the right hemisphere, in DS. This happens with a delay compared to the activity shown by FS. This is well in accordance with evidence suggesting that DS is a disturbance of correct motor timing (Etchell et al., 2014), and is also supported by the evidence that behavioral fluency-shaping intervention leads to activations that point towards normalization of abnormal neural patterns (e.g. Neumann et al., 2005, 2003; De Nil et al., 2004; Toyomura et al., 2015, 2011; compare with Fox et al., 1996; Stager et al., 2003). Compatibly, an increase in brain volumes is present in various regions of the right hemisphere in DS (Jäncke et al., 2004), such as the superior temporal gyrus, inferior frontal gyrus, and in sensorimotor regions (Beal et al., 2013, 2007; Cykowski et al., 2008; Jäncke et al., 2004; Kikuchi et al., 2011; Lu et al., 2010b; Sowman et al., 2017). DS may result in a higher asymmetry (i.e. right hemisphere greater than the left one), and/or no leftward asymmetry, in similar regions (compare with Foundas et al., 2004, 2001; Jäncke et al., 2004), but contrasting reports are present (e.g. Gough et al., 2018). Abnormal activations and/or increases in volumes of the right hemisphere are less evident in DS children (e.g. Beal et al., 2013; Chang et al., 2008), further sustaining the vision that changes in these regions may be the result of compensation (e.g. Neumann et al., 2003; Preibisch et al., 2003), which need time to develop. Thus, in the end, abnormalities in the right hemisphere of DS may be the consequence of abnormal functioning of the left one (Chang et al., 2011; Choo et al., 2016). This is also sustained by the fact that DS is characterized by abnormalities in the structure of the left temporal cortex (e.g. Chang et al., 2015; Garnett et al., 2018; Lu et al., 2010b) and by an increase in white matter of specific parts (e.g. anterior) of the corpus callosum (Choo et al., 2016). Sitek et al. (2016) showed that DS is characterized by decreased connectivity in perisylvian regions related to auditory/motor/speech function, although greater connectivity between basal ganglia and temporal cortex (bilaterally) was also observed. The temporal cortex, especially in the right hemisphere, may have a role in the management of temporal sequences, even from a motor/auditory point of view (Bueti, 2011; Bueti et al., 2008; Davis et al., 2009). Thus, higher neural activations of the right hemisphere in DS could be an attempt of the stuttering brain to recover the correct flow of neural events, in order to favor correct activations of motor programs for their prompt/accurate release. The fact that this may happen in DS about 300 ms later than in FS offers the basis for the appearance of stuttering symptoms such as blocks and repetitions, because the realization of speech needs continued and refined preparation/execution of complex motor programs. Again, the evidence that the present findings are not related to speech tasks confirm that DS may also represent a general motor

Table 4
Significant differences between DS and fluent speakers considering ROIs. Significant differences between DS and fluent speakers (FS), considering ROIs, are indicated by reporting means and SD. Trend differences ($p < 0.1$) are in *italic*.

Time window of interest	Center of ROI (BA; MNI x, y, z)	Mean neural activity (TMS – sham)	Statistics	Effect
66–71 ms 75–82 ms	Superior frontal gyrus (6; 0, 6, 66)	0.097 ± 0.21 (DS) 0.441 ± 0.5 (FS); 0.166 ± 0.32 (DS) 0.668 ± 0.68 (FS)	permutation test, p = 0.023; t(26) = 2.39, p = 0.024; Cohen's d = 0.878, large effect size; permutation test, p = 0.018; t(26) = 2.51, p = 0.018; Cohen's d = 0.924, large effect size	DS < FS
91–102 ms	Left precentral gyrus (6L; −60, −5, 35)	0.102 ± 0.25 (DS) 0.516 ± 0.61 (FS); *0.151 ± 0.16 (DS; mean activity of 65–144 ms window)* *0.372 ± 0.37 (FS; mean activity of 65–144 ms window)*	permutation test, p = 0.031; t(26)= 2.34, p = 0.028; Cohen's d = 0.862, large effect size; *permutation test, p = 0.057; t(26) = 2.07, p = 0.049; Cohen's d = 0.756, medium effect size*	DS < FS
99–101 ms	Left inferior parietal lobule (40L; −65, −30, 40)	0.067 ± 0.23 (DS) 0.368 ± 0.44 (FS)	permutation test, p = 0.039; t(26) = 2.27, p = 0.032; Cohen's d = 0.832, large effect size	DS < FS
149–152 ms	Right superior parietal lobule (7R; 30, −70, 55)	0.05 ± 0.24 (DS) 0.311 ± 0.34 (FS)	permutation test, p = 0.029; t(26) = 2.29, p = 0.030; Cohen's d = 0.865, large effect size	DS < FS
263–268 ms 273–280 ms	Right superior temporal gyrus (22R; 65, −15, 5)	0.176 ± 0.19 (DS) 0.037 ± 0.12 (FS); 0.204 ± 0.19 (DS) 0.055 ± 0.12 (FS)	permutation test, p = 0.023; t(26) = 2.39, p = 0.024; Cohen's d = 0.906, large effect size; permutation test, p = 0.016; t(26) = 2.51, p = 0.018; Cohen's d = 0.956, large effect size	DS > FS
265–268 ms 274–277 ms	Right postcentral gyrus (43R; 65, −15, 15)	0.186 ± 0.19 (DS) 0.049 ± 0.11 (FS); 0.202 ± 0.2 (DS) 0.052 ± 0.15 (FS)	permutation test, p = 0.021; t(26) = 2.24, p = 0.034; Cohen's d = 0.904, large effect size; permutation test, p = 0.025; t(26) = 2.29, p = 0.030; Cohen's d = 0.873, large effect size	DS > FS
369–374 ms	Left middle temporal gyrus (21L; −65, −15, −5)	0.015 ± 0.04 (DS) 0.082 ± 0.07 (FS)	permutation test, p = 0.006; t(26) = 2.98, p = 0.006; Cohen's d = 1.133, large effect size	DS < FS
378–380 ms	Right middle temporal gyrus (21R; 65, −15, −5)	0.070 ± 0.09 (DS) −0.009 ± 0.08 (FS)	permutation test, p = 0.017; t(26) = 2.50, p = 0.019; Cohen's d = 0.929, large effect size	DS > FS
378–380 ms 425–427 ms	Right superior temporal gyrus (38R; 55, 10, −15)	0.066 ± 0.09 (DS) −0.012 ± 0.08 (FS); 0.066 ± 0.04 (DS) 0.013 ± 0.05 (FS)	permutation test, p = 0.025; t(26) = 2.35, p = 0.026; Cohen's d = 0.839, large effect size permutation test, p = 0.008; t(26) = 2.85, p = 0.008; Cohen's d = 1.081, large effect size	DS > FS
454–462 ms	Right middle frontal gyrus (6R; 30, 10, 65)	0.124 ± 0.15 (DS) −0.004 ± 0.07 (FS)	permutation test, p = 0.004; t(26)= 2.71, p = 0.012; Cohen's d = 1.132, large effect size	DS > FS
456–463 ms	Superior frontal gyrus (6; 0, 6, 66)	0.128 ± 0.17 (DS) −0.02 ± 0.1 (FS)	permutation test, p = 0.005; t(26) = 2.83, p = 0.009; Cohen's d = 1.081, large effect size	DS > FS

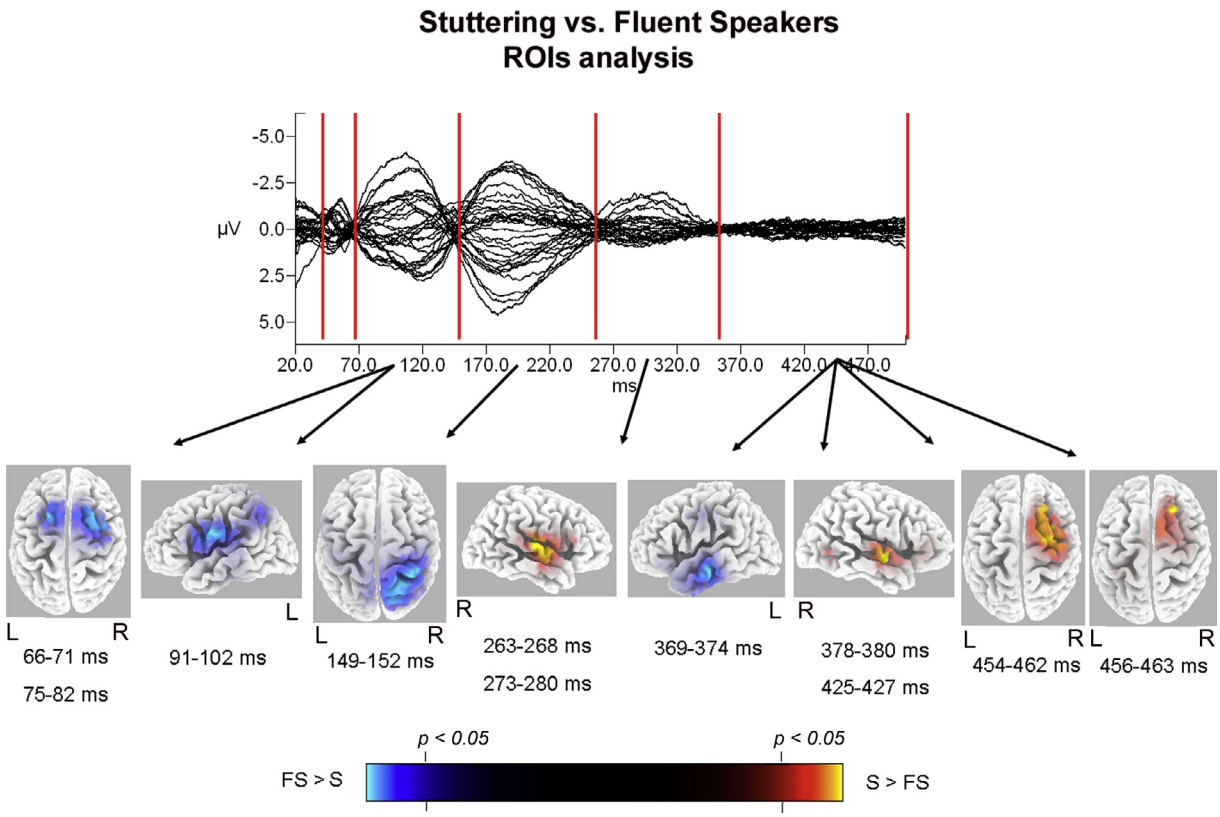

Fig. 6. Representation of significant differences in regions of interest (ROIs) between fluent speakers and stutterers. Significant differences between stutterers and fluent speakers in ROIs are reported with indication of the involved time windows of interest. Blue colors indicate that fluent speakers were more active than stuttering, red/yellow colors indicate that stuttering resulted in higher activation than in fluent speakers. Activations are reported by using relative scales to represent voxels that were significantly activated ($p < 0.05$, corrected); L = left hemisphere, R = right hemisphere. (For interpretation of the references to colour in this figure legend, the reader is referred to the web version of this article.)

deficit (Etchell et al., 2014; Smits-Bandstra and De Nil, 2007). Finally, temporal regions are known to be involved in the elaboration of acoustic information: DS has often been described as a disturbance where impaired/weak/slow integration is evident at the audio-motor level (e.g. Cai et al., 2014a; 2012; Daliri and Max, 2015; Kell et al., 2018; compare with Chang and Zhu, 2013). In line with this, we also report that DS results in lower neural activity in the left temporal cortex (compare with Brown et al., 2005; Kell et al., 2018).

5. Conclusion and future perspectives

The present findings support the hypothesis that DS is a disconnection syndrome where large-scale deficits in neural networks are present. They may be part of a stuttering "trait" (see Budde et al., 2014), but, more importantly, could be related to DS symptoms (i.e. stuttering "state"; compare with Connally et al., 2018): some abnormalities may be the cause and/or the consequence of speech dysfluency, while other may reflect an attempt to overcome it. Speech/motor skills rely on widely distributed systems of brain regions that exchange information in a rapid and synchronized manner. Neural impairment anywhere at this level could result in motor difficulties, such as stuttering, but also in slower and/or more variable motor/speech initiation/execution (e.g. Adams and Hayden, 1976; Bakker and Brutten, 1989; Hillman and Gilbert, 1977; Peters et al., 1989; Zimmermann, 1980) and in higher timing asynchrony (van de Vorst and Gracco, 2017). The differences in neural dynamics between the stuttering brain and FS seen herein, sustain the suggestion that "time" (i.e. an effective neural synchronization and exchange of information between different regions) is a fundamental aspect in DS and that dysfunctions in neural systems are at the basis for the appearance/maintenance of DS symptoms (Etchell et al., 2014; Ludlow and Loucks, 2003; Neumann et al., 2003; Salmelin et al., 2000). The dysfunctional activation of the SMA may contribute to "delayed"/insufficient activation of motor structures of the left hemisphere, followed by an exaggerated "reaction" of temporal/motor structures of the right one, late in time, interfering with correct motor response initiation (e.g. Webster, 1998, 1993, 1990, 1988; Packman et al., 2007; Smits-Bandstra and De Nil, 2007). Thus, the late activation of the right supplementary motor cortex/premotor area in DS may favor compensation of the previous lack of activity in fronto-temporo-parietal regions of the left hemisphere. This "re-activation" may be an attempt to "re-drive" effective motor firing in DS. Stuttering may be the main symptom of a subtle motor syndrome that is most evident during speech considering that it requires sequential/fast coordination of different muscles. The present findings support this vision: speech may be related with increased neural requests, thus leading to higher variability in speech/motor coordination (see Smith and Weber, 2017; Usler et al., 2017). Taken together, these results may have a role in suggesting new and more focused rehabilitative solutions for persistent DS. Non-invasive behavioral and neuro-modulation methods could be used in the attempt to modulate activity in the defective hubs of the DS neural networks (e.g. Chesters et al., 2017, 2018; Yada et al., 2018).

In conclusion, the findings from the present study: (i) provide a functional counterpart to the previously demonstrated white matter abnormalities in DS, especially those close to left inferior frontal cortex, even at a wider network level; (ii) suggest that white matter abnormalities and dysfunctions of the cortico-basal-thalamo-

cortical system (where SMA is one of the main components) in DS could be more overlapping than previously known; (iii) propose a mechanism by which regions of the right hemisphere, usually considered as "compensatory" in DS, "react" to difficulties, i.e. as a consequence of deficient motor activation of structures of the left hemisphere; (iv) sustain the vision of DS as a general motor disorder and a motor timing disorder, wherein the system is not able to promptly respond to neural requests, thus impairing communication in larger networks; (v) propose dynamic mechanisms that can justify the presence of DS symptoms; (vi) propose the SMA as a possible target for neuro-rehabilitation of DS.

Acknowledgments

The authors are grateful to Dr. Marco Zanon and Dr. Luca Weis for useful preliminary discussion and to Dr. Katie Palmer and Dr. Patrick Moore for linguistic revision.

Conflict of interest

None of the authors have potential conflicts of interest to be disclosed.

Funding

This work was supported by Beneficentia Stiftung (Vaduz, Liechtenstein; grant to P.P.B. and P.B.). The funding source had no role in the study.

Appendix A. Supplementary material

Supplementary data to this article can be found online at https://doi.org/10.1016/j.clinph.2018.10.005.

References

Abe K, Yokoyama R, Yorifji S. On stuttering-like hesitation resulting from infarct in the midbrain and the mesial thalami. Rinsho Shinkeigaku 1992;32:822–5.
Abe K, Yokoyama R, Yorifuji S. Repetitive speech disorder resulting from infarcts in the paramedian thalami and midbrain. J Neurol Neurosurg Psychiatry 1993;56:1024–6.
Ackermann H, Hertrich I, Ziegler W, Bitzer M, Bien S. Acquired dysfluencies following infarction of the left mesiofrontal cortex. Aphasiology 1996;10:409–17.
Adams MR, Hayden P. The ability of stutterers and nonstutterers to initiate and terminate phonation during production of an isolated vowel. J Speech Hear Res 1976;19:290–6.
Alexander M, Naeser M, Palumbo C. Correlations of subcortical CT lesion sites and aphasia profiles. Brain 1987;110:961–91.
Alm PA. Stuttering and the basal ganglia circuits: a critical review of possible relations. J Commun Disord 2004;37:325–69.
Arcara G, Petrova A. erpR: event-related potentials (ERP) analysis, graphics and utility functions (R package version 0.2.0); 2017. Available from: <http://CRAN.R-project.org/package=erpR>.
Avanzino L, Pelosin E, Vicario CM, Lagravinese G, Abbruzzese G, Martino D. Time processing and motor control in movement disorders. Front Hum Neurosci 2016;10:631.
Bakker K, Brutten GJ. A comparative investigation of the laryngeal premotor, adjustment, and reaction times of stutterers and nonstutterers. J Speech Hear Res 1989;32:239–44.
Beal DS, Gracco VL, Brettschneider J, Kroll RM, De Nil LF. A voxel-based morphometry (VBM) analysis of regional grey and white matter volume abnormalities within the speech production network of children who stutter. Cortex 2013;49:2151–61.
Beal DS, Gracco VL, Lafaille SJ, DeNil LF. Voxel-based morphometry of auditory and speech-related cortex in stutterers. Neuroreport 2007;18:1257–60.
Beal DS, Lerch JP, Cameron B, Henderson R, Gracco V, De Nil LF. The trajectory of grey matter development in Broca's area is abnormal in people who stutter. Front Hum Neurosci 2015;9:89.
Belyk M, Kraft SJ, Brown S. Stuttering as a trait or state-an ALE meta-analysis of neuroimaging studies. Eur J Neurosci 2015;41:275–84.
Braun AR, Varga M, Stager S, Schulz G, Selbie S, Maisog JM, et al. Altered patterns of cerebral activity during speech and language production in developmental stuttering. An H2(15)O positron emission tomography study. Brain 1997;120:761–84.
Brown S, Ingham RJ, Ingham JC, Laird AR, Fox PT. Stuttered and fluent speech production: an ALE meta-analysis of functional neuroimaging studies. Hum Brain Mapp 2005;25:105–17.
Budde KS, Barron DS, Fox PT. Stuttering, induced fluency, and natural fluency: a hierarchical series of activation likelihood estimation meta-analyses. Brain Lang 2014;139:99–107.
Bueti D. The sensory representation of time. Front Integr Neurosci 2011;5:34.
Bueti D, van Dongen EV, Walsh V. The role of superior temporal cortex in auditory timing. PLoS One 2008;3:e2481.
Busan P, Battaglini PP, Sommer M. Transcranial magnetic stimulation in developmental stuttering: relations with previous neurophysiological research and future perspectives. Clin Neurophysiol 2017;128:952–64.
Busan P, Battaglini PP, Borelli M, Evaristo P, Monti F, Pelamatti G. Investigating the efficacy of paroxetine in developmental stuttering. Clin Neuropharmacol 2009;32:183–8.
Busan P, D'Ausilio A, Borelli M, Monti F, Pelamatti G, Pizzolato G, et al. Motor excitability evaluation in developmental stuttering: a transcranial magnetic stimulation study. Cortex 2013;49:781–92.
Busan P, Del Ben G, Bernardini S, Natarelli G, Bencich M, Monti F, et al. Altered modulation of silent period in tongue motor cortex of persistent developmental stuttering in relation to stuttering severity. PLoS One 2016;11:e0163959.
Cai S, Beal DS, Ghosh SS, Guenther FH, Perkell JS. Impaired timing adjustment in response to time-varying auditory perturbation during connected speech production in persons who stutter. Brain Lang 2014a;129:24–9.
Cai S, Beal DS, Gosh SS, Tiede MK, Guenther FH, Perkell JS. Weak responses to auditory feedback perturbation during articulation in persons who stutter: evidence for abnormal auditory-motor transformation. PLoS One 2012;7:e41830.
Cai S, Tourville JA, Beal DS, Perkell JS, Guenther FH, Ghosh SS. Diffusion imaging of cerebral white matter in persons who stutter: evidence for network-level anomalies. Front Hum Neurosci 2014b;8:54.
Cantello R, Tarletti R, Civardi C. Transcranial magnetic stimulation and Parkinson's disease. Brain Res Rev 2002;38:309–27.
Chang SE, Zhu DC. Neural network connectivity differences in children who stutter. Brain 2013;136:3709–26.
Chang SE, Zhu DC, Choo AL, Angstadt M. White matter neuroanatomical differences in young children who stutter. Brain 2015;138:694–711.
Chang SE, Chow HM, Wieland EA, McAuley JD. Relation between functional connectivity and rhythm discrimination in children who do and do not stutter. Neuroimage Clin 2016;12:442–50.
Chang SE, Erickson KI, Ambrose NG, Hasegawa-Johnson MA, Ludlow CL. Brain anatomy differences in childhood stuttering. Neuroimage 2008;39:1333–44.
Chang SE, Horwitz B, Ostuni J, Reynolds R, Ludlow CL. Evidence of left inferior frontal-premotor structural and functional connectivity deficits in adults who stutter. Cereb Cortex 2011;21:2507–18.
Chesters J, Möttönen R, Watkins KE. Transcranial direct current stimulation over left inferior frontal cortex improves speech fluency in adults who stutter. Brain 2018;141:1161–71.
Chesters J, Watkins KE, Möttönen R. Investigating the feasibility of using transcranial direct current stimulation to enhance fluency in people who stutter. Brain Lang 2017;164:68–76.
Choo AL, Burnham E, Hicks K. Chang SE Dissociations among linguistic, cognitive, and auditory-motor neuroanatomical domains in children who stutter. J Commun Disord 2016;6:29–47.
Chow HM, Chang SE. White matter developmental trajectories associated with persistence and recovery of childhood stuttering. Hum Brain Mapp 2017;38:3345–59.
Chung SJ, Im JH, Lee JH, Lee MC. Stuttering and gait disturbance after supplementary motor area seizure. Mov Disord 2004;19:1106–9.
Cieslak M, Ingham RJ, Ingham JC, Grafton ST. Anomalous white matter morphology in adults who stutter. J Speech Lang Hear Res 2015;58:268–77.
Civier O, Bullock D, Max L, Guenther FH. Computational modeling of stuttering caused by impairments in a basal ganglia thalamo-cortical circuit involved in syllable selection and initiation. Brain Lang 2013;126:263–78.
Civier O, Kronfeld-Duenias V, Amir O, Ezrati-Vinacour R, Ben-Shachar M. Reduced fractional anisotropy in the anterior corpus callosum is associated with reduced speech fluency in persistent developmental stuttering. Brain Lang 2015;143:20–31.
Civier O, Tasko SM, Guenther FH. Overreliance on auditory feedback may lead to sound/syllable repetitions: simulations of stuttering and fluency-inducing conditions with a neural model of speech production. J Fluency Disord 2010;35:246–79.
Clos M, Amunts K, Laird AR, Fox PT, Eickhoff SB. Tackling the multifunctional nature of Broca's region meta-analytically: co-activation-based parcellation of area 44. Neuroimage 2013;83:174–88.
Cohen J. Statistical power analysis for the behavioral sciences. 2nd ed. Hillsdale: Lawrence Erlbaum; 1988.
Cona G, Semenza C. Supplementary motor area as key structure for domain-general sequence processing: a unified account. Neurosci Biobehav Rev 2017;72:28–42.
Connally EL, Ward D, Howell P, Watkins KE. Disrupted white matter in language and motor tracts in developmental stuttering. Brain Lang 2014;131:25–35.
Connally EL, Ward D, Pilatsikas C, Finnegan S, Jenkinson M, Boyles R, et al. Separation of trait and state in stuttering. Hum Brain Mapp 2018. https://doi.org/10.1002/hbm.24063.

Coull JT, Charras P, Donadieu M, Droit-Volet S, Vidal F. SMA selectively codes the active accumulation of temporal, not spatial, magnitude. J Cogn Neurosci 2015;27:2281–98.
Craig-McQuaide A, Akram H, Zrinzo L, Tripoliti E. A review of brain circuitries involved in stuttering. Front Hum Neurosci 2014;8:884.
Cykowski MD, Fox PT, Ingham RJ, Ingham JC, Robin DA. A study of the reproducibility and etiology of diffusion anisotropy differences in developmental stuttering: a potential role for impaired myelination. Neuroimage 2010;52:1495–504.
Cykowski MD, Kochunov PV, Ingham RJ, Ingham JC, Mangin JF, Rivière D, et al. Perysilvian sulcal morphology and cerebral asymmetry patterns in adults who stutter. Cereb Cortex 2008;18:571–83.
Daliri A, Max L. Modulation of auditory processing during speech movement planning is limited in adults who stutter. Brain Lang 2015;143:59–68.
Davis B, Christie J, Rorden C. Temporal order judgements activate temporal parietal junction. J Neurosci 2009;29:3182–8.
De Nil LF, Kroll RM, Lafaille SJ, Houle S. A positron emission tomography study of short-and long-term treatment effects on functional brain activation in adults who stutter. J Fluency Disord 2004;28:357–80.
Delorme A, Makeig S. EEGLAB: an open source toolbox for analysis of single-trial EEG dynamics including independent component analysis. J Neurosci Methods 2004;134:9–21.
Desai J, Huo Y, Wang Z, Bansal R, Williams SC, Lythgoe D, et al. Reduced perfusion in Broca's area in developmental stuttering. Hum Brain Mapp 2017;38:1865–74.
Duann JR, Ide JS, Luo X, Li CS. Functional connectivity delineates distinct roles of the inferior frontal cortex and presupplementary motor area in stop signal inhibition. J Neurosci 2009;29:10171–9.
Ellis P. The essential guide to effect sizes: statistical power, meta-analysis, and the interpretation of research results. Cambridge: Cambridge University Press; .
Etchell AC, Civier O, Ballard K, Sowman PF. A systematic literature review of neuroimaging research on developmental stuttering between 1995 and 2016. J Fluency Disord 2018;55:6–45.
Etchell AC, Johnson BW, Sowman PF. Behavioral and multimodal neuroimaging evidence for a deficit in brain timing networks in stuttering: a hypothesis and theory. Front Hum Neurosci 2014;8:467.
Exner C, Koschack J, Irle E. The differential role of premotor frontal cortex and basal ganglia in motor sequence learning: evidence from focal basal ganglia lesions. Learn Mem 2002;9:376–86.
Foundas AL, Bollich AM, Corey DM, Hurley M, Heilman KM. Anomalous anatomy of speech-language areas in adults with persistent developmental stuttering. Neurology 2001;57:207–15.
Foundas AL, Bollich AM, Feldman J, Corey DM, Hurley M, Lemen LC, et al. Aberrant auditory processing and atypical planum temporale in developmental stuttering. Neurology 2004;63:1640–6.
Fox PT, Ingham RJ, Ingham JC, Hirsch TB, Downs JH, Martin C, et al. A PET study of the neural systems of stuttering. Nature 1996;382:158–61.
Fox PT, Ingham RJ, Ingham JC, Zamarripa F, Xiong JH, Lancaster JL. Brain correlates of stuttering and syllable production. A PET performance-correlation analysis. Brain 2000;123:1985–2004.
Garnett EO, Chow HM, Nieto-Castanon A, Tourville JA, Guenther FH, Chang SE. Anomalous morphology in left hemisphere motor and premotor cortex of children who stutter. Brain 2018. https://doi.org/10.1093/brain/awy199.
Gough PM, Connally EL, Howell P, Ward D, Chesters J, Watkins KE. Planum temporale asymmetry in people who stutter. J Fluency Disord 2018;55:94–105.
Hartwigsen G, Saur D, Price CJ, Ulmer S, Baumgaertner A, Siebner HR. Perturbation of the left inferior frontal gyrus triggers adaptive plasticity in the right homologous area during speech production. Proc Natl Acad Sci USA 2013;110:16402–7.
Hedges LV, Olkin I. Statistical methods for meta-analysis. Academic Press, London; 1985.
Hertrich I, Dietrich S, Ackermann H. The role of the supplementary motor area for speech and language processing. Neurosci Biobehav Rev 2016;68:602–10.
Hickok G, Okada K, Serences JT. Area Spt in the human planum temporale supports sensory-motor integration for speech processing. J Neurophysiol 2009;101:2725–32.
Hill AT, Rogasch NC, Fitzgerald PB, Hoya KE. TMS-EEG: a window into the neurophysiological effects of transcranial electrical stimulation in non-motor brain regions. Neurosci Biobehav Rev 2016;64:175–84.
Hillman RE, Gilbert HR. Voice onset time for voiceless stop consonants in the fluent reading of stutterers and nonstutterers. J Acoust Soc Am 1977;61:610–1.
Howell P. Assessment of some contemporary theories of stuttering that apply to spontaneous speech. Contemp Issues Commun Sci Disord 2004;31:122–39.
Ilmoniemi RJ. TMS-EEG: methodology. Clin Neuropysiol 2016;127:e21.
Ingham RJ, Fox PT, Ingham JC, Zamarripa F, Martin C, Jerabek P, et al. Functional-lesion investigation of developmental stuttering with positron emission tomography. J Speech Hear Res 1996;39:1208–27.
Ingham RJ, Grafton ST, Bothe AK, Ingham JC. Brain activity in adults who stutter: similarities across speaking tasks and correlations with stuttering frequency and speaking rate. Brain Lang 2012;122:11–24.
Jäncke L, Hänggi J, Steinmetz H. Morphological brain differences between adult stutterers and nonstutterers. BMC Neurol 2004;4:23.
Jung TP, Makeig S, Humphries C, Lee TW, McKeown MJ, Iragui V, et al. Removing electroencephalographic artifacts by blind source separation. Psychophysiology 2000;37:163–78.
Kell CA, Neumann K, Behrens M, von Gudenberg AW, Giraud L. Speaking-related changes in cortical functional connectivity associated with assisted and spontaneous recovery from developmental stuttering. J Fluency Disord 2018;55:135–44.
Kell CA, Neumann K, von Kriegstein K, Posenenske C, von Gudenberg AW, Euler H, et al. How the brain repairs stuttering. Brain 2009;132:2747–60.
Kemerdere R, de Champfleur NM, Deverdun J, Cochereau J, Moritz-Gasser S, Herbet G, et al. Role of the left frontal aslant tract in stuttering: a brain stimulation and tractographic study. J Neurol 2016;263:157–67.
Kikuchi Y, Ogata K, Umesaki T, Yoshiura T, Kenjo M, Hirano Y, et al. Spatiotemporal signatures of an abnormal auditory system in stuttering. Neuroimage 2011;55:891–9.
Kinoshita M, de Champfleur NM, Deverdun J, Moritz-Gasser S, Herbet G, Duffau H. Role of frontostriatal tract and frontal aslant tract in movement and speech: an axonal mapping study. Brain Struct Funct 2015;220:3399–412.
Kronfeld-Duenias V, Amir O, Ezrati-Vinacour R, Civier O, Ben-Shachar M. The frontal aslant tract underlies speech fluency in persistent developmental stuttering. Brain Struct Funct 2016;221:365–81.
Lodish H, Berk A, Zipursky SL, Matsudaira P, Baltimore D, Darnell J. Molecular Cell Biology. 4th ed. New York: WH Freeman; 2000.
Lu C, Chen C, Ning N, Ding G, Guo T, Peng D, et al. The neural substrates for atypical planning and execution of word production in stuttering. Exp Neurol 2010a;221:146–56.
Lu C, Chen C, Peng D, You W, Zhang X, Ding G, et al. Neural anomaly and reorganization in speakers who stutter: a short-term intervention study. Neurology 2012;79:625–32.
Lu C, Ning N, Peng D, Ding G, Li K, Yang Y, et al. The role of large-scale neural interactions for developmental stuttering. Neuroscience 2009;161:1008–26.
Lu C, Peng D, Chen C, Ning N, Ding G, Li K, et al. Altered effective connectivity and anomalous anatomy in the basal ganglia-thalamocortical circuit of stuttering speakers. Cortex 2010b;46:49–67.
Ludlow CL, Loucks T. Stuttering: a dynamic motor control disorder. J Fluency Disord 2003;28:273–95.
Massimini M, Ferrarelli F, Huber R, Esser SK, Singh H, Tononi G. Breakdown of cortical effective connectivity during sleep. Science 2005;309:2228–32.
Max L, Guenther FH, Gracco VL, Ghosh SS, Wallace ME. Unstable or insufficiently activated internal models and feedback-biased motor control as sources of dysfluency: a theoretical model of stuttering. Contemp Issues Commun Sci Disord 2004;31:105–22.
Metzger FL, Auer T, Helms G, Paulus W, Frahm J, Sommer M, et al. Shifted dynamic interactions between subcortical nuclei and inferior frontal gyri during response preparation in persistent developmental stuttering. Brain Struct Funct 2018;223:165–82.
Miniussi C, Harris JA, Ruzzoli M. Modelling non-invasive brain stimulation in cognitive neuroscience. Neurosci Biobehav Rev 2013;37:1702–12.
Miniussi C, Paulus W, Rossini PM. Transcranial brain stimulation. Boca Raton: CRC Press; 2012.
Misaghi E, Zhang Z, Gracco VL, De Nil LF, Beal DS. White matter tractography of the neural network for speech-motor control in children who stutter. Neurosci Lett 2018;668:37–42.
Mita A, Mushiake H, Shima K, Matsuzaka Y, Tanji J. Interval time coding by neurons in the presupplementary motor areas. Nat Neurosci 2009;12:502–7.
Nachev P, Kennard C, Husain M. Functional role of the supplementary and pre-supplementary motor areas. Nat Rev Neurosci 2008;9:856–69.
Nakamura K, Sakai K, Hikosaka O. Neuronal activity in medial frontal cortex during learning of sequential procedures. J Neurophysiol 1998;80:2671–87.
Narayana S, Laird AR, Tandon N, Franklin C, Lancaster JL, Fox PT. Electrophysiological and functional connectivity of the human supplementary motor area. Neuroimage 2012;62:250–65.
Neef NE, Anwander A, Bütfering C, Schmidt-Samoa C, Friederici AD, Paulus W, et al. Structural connectivity of right frontal hyperactive areas scales with stuttering severity. Brain 2018;141:191–204.
Neef NE, Anwander A, Friederici AD. The neurobiological grounding of persistent stuttering: from structure to function. Curr Neurol Neurosci Rep 2015a;15:63.
Neef NE, Bütfering C, Anwander A, Friederici AD, Paulus W, Sommer M. Left posterior-dorsal area 44 couples with parietal areas to promote speech fluency, while right area 44 activity promotes the stopping of motor responses. Neuroimage 2016;142:628–44.
Neef NE, Hoang TN, Neef A, Paulus W, Sommer M. Speech dynamics are coded in the left motor cortex in fluent speakers but not in adults who stutter. Brain 2015b;138:712–25.
Neef NE, Paulus W, Neef A, von Gudenberg AW, Sommer M. Reduced intracortical inhibition and facilitation in the primary motor tongue representation of adults who stutter. Clin Neurophysiol 2011;122:1802–11.
Neumann K, Euler HA, von Gudenberg AW, Giraud AL, Lanfermann H, Gall V, et al. The nature and treatment of stuttering as revealed by fMRI. A within- and between group comparison. J Fluency Disord 2003;28:381–409.
Neumann K, Preibisch C, Euler HA, von Gudenberg AW, Lanfermann H, Gall V, et al. Cortical plasticity associated with stuttering therapy. J Fluency Disord 2005;30:23–39.
Nichols TE, Holmes PA. Nonparametric permutation tests for functional neuroimaging; a primer with examples. Hum Brain Mapp 2002;15:1–25.
Nikulin VV, Kicic D, Kahkonen S, Ilmoniemi RJ. Modulation of electroencephalographic responses to transcranial magnetic stimulation: evidence for changes in cortical excitability related to movement. Eur J Neurosci 2003;18:1206–12.

Nikulin V, Ruohonen J, Ilmoniemi R. The role of the coil click in TMS assessed with simultaneous EEG. Clin Neurophysiol 1999;110:1325–8.
Oldfield RC. The assessment and analysis of handedness: the Edinburgh Inventory. Neuropsychologia 1971;9:97–113.
Packman A, Code C, Onslow M. On the cause of stuttering: integrating theory with brain and behavioral research. J Neurolinguistics 2007;20:353–62.
Pascual-Marqui RD. Standardized low resolution brain electromagnetic tomography: a new method for localizing electrical activity in the brain. Int J Psychophysiol 2002;18:49–65.
Penfield W, Welch K. The supplementary motor area of the cerebral cortex; a clinical and experimental study. JAMA Arch Neurol Psychiatry 1951;66:289–317.
Peters HF, Hulstijn W, Starkweather CW. Acoustic and physiological reaction times of stutterers and nonstutterers. J Speech Hear Res 1989;32:668–80.
Preibisch C, Neumann K, Raab P, Euler HA, von Gudenberg AW, Lanfermann H, et al. Evidence for compensation for stuttering by the right frontal operculum. Neuroimage 2003;20:1356–64.
Premoli I, Castellanos N, Rivolta D, Belardinelli P, Bajo R, Zipser C, Espenhahn S, Heidegger T, Muller-Dahlhaus F, Ziemann U. TMS-EEG signatures of GABAergic neurotransmission in the human cortex. J Neurosci 2014;34:5603–12.
Qiao J, Wang Z, Zhao G, Huo Y, Herder CL, Sikora CO, et al. Functional neural circuits that underlie developmental stuttering. PLoS One 2017;12:e0179255.
Restle J, Murakami T, Ziemann U. Facilitation of speech repetition accuracy by theta burst stimulation of the left posterior inferior frontal gyrus. Neuropsychologia 2012;50:2026–31.
Riley G. The stuttering severity instrument for adults and children (SSI-4). 4th ed. Austin: PRO-ED; 2009.
Rogasch NC, Daskalakis ZJ, Fitzgerald PB. Cortical inhibition of distinct mechanisms in the dorsolateral prefrontal cortex is related to working memory performance: a TMS-EEG study. Cortex 2015;64:68–77.
Salmelin R, Schnitzler A, Schmitz F, Freund HJ. Single word reading in developmental stutterers and fluent speakers. Brain 2000;123:1184–202.
Sekiguchi H, Takeuchia S, Kadotac H, Kohnob Y, Nakajima Y. TMS-induced artifacts on EEG can be reduced by rearrangement of the electrode's lead wire before recording. Clin Neurophysiol 2011;122:984–90.
Shima K, Tanji J. Binary-coded monitoring of a behavioral sequence by cells in the pre-supplementary motor area. J Neurosci 2006;26:2579–82.
Shima K, Mushiake H, Saito N, Tanji J. Role for cells in the presupplementary motor area in updating motor plans. Proc Natl Acad Sci USA 1996;93:8694–8.
Sitek KR, Cai S, Beal DS, Perkell JS, Guenther FH, Ghosh SS. Decreased cerebellar-orbito-frontal connectivity correlates with stuttering severity: whole-brain functional and structural connectivity associations with persistent developmental stuttering. Front Hum Neurosci 2016;10:190.
Smith A, Weber C. How stuttering develops: the multifactorial dynamic pathways theory. J Speech Lang Hear Res 2017;60:2483–505.
Smits-Bandstra S, De Nil LF. Sequence skill learning in persons who stutter: implications for corticostriato-thalamo-cortical dysfunction. J Fluency Disord 2007;32:251–78.
Sommer M, Koch MA, Paulus W, Weiller C, Büchel C. Disconnection of speech-relevant brain areas in persistent developmental stuttering. Lancet 2002;360:380–3.
Sowman PF, Ryan M, Johnson BW, Savage G, Crain S, Harrison E, et al. Grey matter volume differences in the left caudate nucleus of people who stutter. Brain Lang 2017;164:9–15.
Stager SV, Jeffries KJ, Braun AR. Common features of fluency-evoking conditions studied in stuttering subjects and controls: an H(2)15O PET study. J Fluency Disord 2003;28:319–35.
Tanji J, Shima K. Role for supplementary motor area cells in planning several movements ahead. Nature 1994;371:413–6.
Tanji J, Shima K. Supplementary motor cortex in organization of movement. Eur Neurol 1996;36:13–9.
Toyomura A, Fujii T, Kuriki S. Effect of external auditory pacing on the neural activity of stuttering speakers. Neuroimage 2011;57:1507–16.
Toyomura A, Fujii T, Kuriki S. Effect of an 8-week practice of externally triggered speech on basal ganglia activity of stuttering and fluent speakers. Neuroimage 2015;109:458–68.
Usler E, Smith A, Weber C. A lag in speech motor coordination during sentence production is associated with stuttering persistence in young children. J Speech Lang Hear Res 2017;60:51–61.
Van de Vorst R, Gracco VL. Atypical non-verbal sensorimotor synchronization in adults who stutter may be modulated by auditory feedback. J Fluency Disord 2017;53:14–25.
Veniero D, Bortoletto M, Miniussi C. TMS-EEG co-registration: on TMS-induced artifact. Clin Neurophysiol 2009;120:1392–9.
Watkins KE, Smith SM, Davis S, Howell P. Structural and functional abnormalities of the motor system in developmental stuttering. Brain 2008;131:50–9.
Webster WG. Brain models and the clinical management of stuttering. Can J Speech Lang Pathol Audiol 1998;22:220–30.
Webster WG. Motor performance of stutterers: a search for mechanisms. J Mot Behav 1990;22:553–71.
Webster WG. Hurried hands and tangled tongues. In: Boberg E, editor. Neuropsychology of stuttering. Edmonton: The University of Alberta Press; 1993. p. 73–127.
Webster WG. Neural mechanisms underlying stuttering: evidence from bimanual handwriting performance. Brain Lang 1988;33:226–44.
Wu JC, Maguire G, Riley G, Lee A, Keator D, Tang C, et al. Increased dopamine activity associated with stuttering. Neuroreport 1997;8:767–70.
Whillier A, Hommel S, Neef NE, von Gudenberg AW, Paulus W, Sommer M. Adults who stutter lack the specialized pre-speech facilitation found in non-stutterers. PLoS ONE 2018;13.
Yada Y, Tomisato S, Hashimoto RI. Online cathodal transcranial direct current stimulation to the right homologue of Broca's area improves speech fluency in people who stutter. Psychiatry Clin Neurosci 2018. https://doi.org/10.1111/pcn.12796.
Yang Y, Jia F, Siok WT, Tan LH. Altered functional connectivity in persistent developmental stuttering. Sci Rep 2016;6:19128.
Zanon M, Battaglini PP, Jarmolowska J, Pizzolato G, Busan P. Long-range neural activity evoked by premotor cortex stimulation: a TMS/EEG co-registration study. Front Hum Neurosci 2013;7:803.
Zanon M, Busan P, Monti F, Pizzolato G, Battaglini PP. Cortical connections between dorsal and ventral visual streams in humans: evidence by TMS/EEG co-registration. Brain Topogr 2010;22:307–17.
Zhang S, Ide JS, Li CR. Resting-state functional connectivity of the medial superior frontal cortex. Cereb Cortex 2012;22:99–111.
Ziemann U, Tergau F, Bruns D, Baudewig J, Paulus W. Changes in human motor cortex excitability induced by dopaminergic and antidopaminergic drugs. Electroenceph Clin Neurophysiol 1997;105:430–7.
Zimmermann G. Articulatory dynamics of fluent utterances of stutterers and nonstutterers. J Speech Hear Res 1980;23:95–107.
Zanon M, Borgomaneri S, Avenanti A. Action-related dynamic changes in inferior frontal cortex effective connectivity: A TMS/EEG coregistration study. Cortex 2018;108:193–209.